

AD A 093502

(12) LEVEL *III*

AD-E430553

AD

TECHNICAL REPORT ARBRL-TR-02271

IMPACT DYNAMICS: THEORY AND EXPERIMENT

J. A. Zukas

October 1980

DTIC  
ELECTED  
JAN 6 1981  
S D  
B



US ARMY ARMAMENT RESEARCH AND DEVELOPMENT COMMAND  
BALLISTIC RESEARCH LABORATORY  
ABERDEEN PROVING GROUND, MARYLAND

Approved for public release; distribution unlimited.

DDC FILE COPY

80 12 18 039

Destroy this report when it is no longer needed.  
Do not return it to the originator.

Secondary distribution of this report by originating  
or sponsoring activity is prohibited.

Additional copies of this report may be obtained  
from the National Technical Information Service,  
U.S. Department of Commerce, Springfield, Virginia  
22151.

The findings in this report are not to be construed as  
an official Department of the Army position, unless  
so designated by other authorized documents.

*The use of trade names or manufacturers' names in this report  
does not constitute endorsement of any commercial product.*

## UNCLASSIFIED

SECURITY CLASSIFICATION OF THIS PAGE (When Data Entered)

REPORT DOCUMENTATION PAGE		READ INSTRUCTIONS BEFORE COMPLETING FORM
1. REPORT NUMBER	2. GOVT ACCESSION NO.	3. RECIPIENT'S CATALOG NUMBER
TECHNICAL REPORT ARBRL-TR-02271		AD A093502
4. TITLE (and Subtitle)	5. TYPE OF REPORT & PERIOD COVERED	
IMPACT DYNAMICS: THEORY AND EXPERIMENT	Final	
7. AUTHOR(s)	6. PERFORMING ORG. REPORT NUMBER	
J. A. Zukas	8. CONTRACT OR GRANT NUMBER(s)	
9. PERFORMING ORGANIZATION NAME AND ADDRESS U.S. Army Ballistic Research Laboratory (ATTN: DRDAR-BLT) Aberdeen Proving Ground, MD 21005	10. PROGRAM ELEMENT, PROJECT, TASK AREA & WORK UNIT NUMBERS 1L162618AH80	
11. CONTROLLING OFFICE NAME AND ADDRESS U.S. Army Armament Research and Development Command U.S. Army Ballistic Research Laboratory (ATTN: DRDAR-BL) Aberdeen Proving Ground, MD 21005	12. REPORT DATE OCTOBER 1980	
14. MONITORING AGENCY NAME & ADDRESS (if different from Controlling Office)	13. NUMBER OF PAGES 67	
	15. SECURITY CLASS. (of this report) UNCLASSIFIED	
	15a. DECLASSIFICATION/DOWNGRADING SCHEDULE	
16. DISTRIBUTION STATEMENT (of this Report) Approved for public release, distribution unlimited.		
17. DISTRIBUTION STATEMENT (of the abstract entered in Block 20, if different from Report)		
18. SUPPLEMENTARY NOTES		
19. KEY WORDS (Continue on reverse side if necessary and identify by block number)		
Impact Dynamics Terminal Ballistics Dynamic Fracture Penetration & Perforation	Wave Propagation Impulse Loading Structural Dynamics	
20. ABSTRACT (Continue on reverse side if necessary and identify by block number) (h1b)		
A review is presented of the state of the art in the analysis of materials and structures subjected to intense impulsive loading. Emphasis is placed on the penetration and perforation of solids and current developments in three-dimensional finite element and finite difference simulation of impact phenomena. The need for adequate characterization of material response and failure at high strain rates is emphasized and current capabilities highlighted. An assessment is made of anticipated developments and advances in high speed computers, high (continued)		

UNCLASSIFIED

SECURITY CLASSIFICATION OF THIS PAGE(When Data Entered)

strain rate materials characterization, and in numerical simulation techniques which will contribute to improved design and reduced vulnerability of materials and structures to impact loading.

UNCLASSIFIED

SECURITY CLASSIFICATION OF THIS PAGE(When Data Entered)

TABLE OF CONTENTS

	Page
LIST OF ILLUSTRATIONS . . . . .	5
I. INTRODUCTION . . . . .	7
A. General. . . . .	7
B. Penetration & Perforation of Solids. . . . .	9
II. NUMERICAL SIMULATION OF IMPACT PHENOMENA . . . . .	17
A. General Considerations . . . . .	17
B. Discretization Methods . . . . .	21
C. Mesh Descriptions. . . . .	23
D. Temporal Integration Schemes . . . . .	25
E. Computer Resource Requirements . . . . .	28
F. Material Model . . . . .	29
III. CURRENT CODE CAPABILITIES. . . . .	32
A. Two-Dimensional Lagrangian Codes . . . . .	32
B. Two-Dimensional Eulerian Codes . . . . .	33
C. Three-Dimensional Codes. . . . .	35
IV. EXAMPLES . . . . .	37
A. Sphere Ricochet. . . . .	37
B. Yawed Rod Impact . . . . .	40
C. Hydrodynamic Ram . . . . .	42
V. COMPUTATIONAL FAILURE MODELS . . . . .	43
VI. PROGNOSIS. . . . .	48
REFERENCES . . . . .	53
DISTRIBUTION LIST. . . . .	61

## LIST OF ILLUSTRATIONS

Figure	Page
1. Failure modes in impacted plates. . . . .	11
2. Experimental test set-up of x-ray instrumentation for obtaining peretratration data for projectiles. . . .	13
3. Computational process for impact simulation . . . . .	19
4. Lagrangian computational grid . . . . .	24
5. Eulerian computational grid . . . . .	26
6. Deformation profiles for oblique impact of steel sphere into aluminum target at various times. . . . .	33
7. Velocity histories for oblique impact of steel sphere into aluminum target. . . . .	39
8. Rod deformation at various times. . . . .	41
9. Deformations and pressures in fuel tank simulator at 40 and 180 $\mu$ m. . . . .	44

Accession For	
NTIS GRA&I	<input checked="" type="checkbox"/>
DTIC TAB	<input type="checkbox"/>
Unannounced	<input type="checkbox"/>
Justification	
By _____	
Distribution/ _____	
Availability Codes	
Dist	Avail and/or Special
A	

I. INTRODUCTION

## A. General

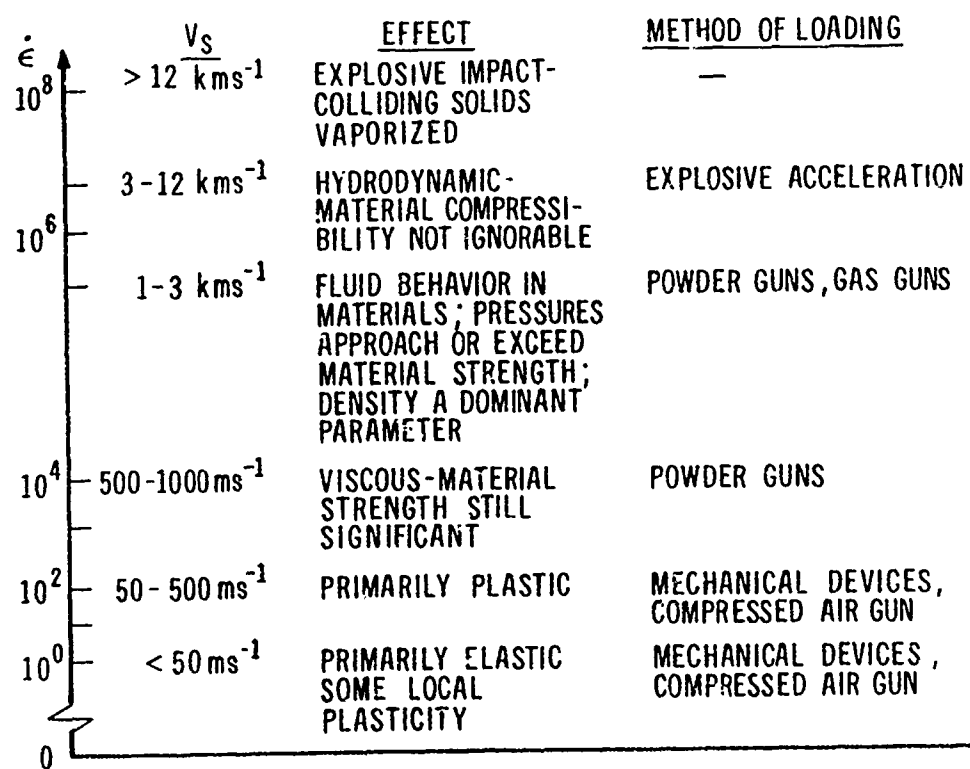
Situations involving impact--the collision of two or more solid bodies-- are currently receiving widespread attention. Traditionally, the prime interest in this area has been for military applications. However, advances in technology have placed such severe demands on materials behavior under short-term loading that current interest in the response of materials and structures to intense impulsive loading centers on such problems as

- transportation safety of hazardous materials
- vehicle crashworthiness
- safety of nuclear reactor structures subjected to impact by tornado-borne debris and aircraft collisions
- the vulnerability of military vehicles, structures, and aircraft to impact and explosive loading
- design of lightweight armor systems
- erosion and fracture of solids due to liquid and solid particle impacts
- protection of spacecraft from meteoroid impact
- explosive forming and welding of metals.

The study of impact phenomena involves a variety of classical disciplines. In the low velocity regime (<2.0 m/s) many problems fall into the area of structural dynamics. Local indentations or penetrations are strongly coupled to the overall deformation of the structure. Frequently, the striker can be replaced, through the Hertz contact theory [1], with an equivalent load distribution acting over a given area in a given time and the analysis of the target performed using conventional structural analysis techniques. Typically, loading and response times are in the millisecond regime. As the striking velocity increases (0.5-1.5 km/s) the response of the structure is dominated by the behavior of the material within a small zone (typically 2-3 projectile diameters) of the impact area. A wave description of the phenomenon is appropriate and the influences of velocity, geometry, material constitution, strain rate, localized plastic flow, and failure are manifest at various stages of the impact process. Typically, loading and reaction times are on the order of microseconds. Still further increases in impact velocity (2-3 km/s) result in localized pressures which exceed by an order of magnitude the strength of the material. In effect the colliding solids can be treated as fluids in the early stages of impact. At ultra-high velocities (>12 km/s) energy deposition occurs at such a high rate that an explosive vaporization of colliding materials results.

Impact phenomena can be characterized in a number of ways: according to the impact angle, the geometric and material characteristics of the target or projectile, or striking velocity. The latter approach is adopted in Table 1 which provides a short classification of impact processes as a function of striking velocity,  $V_s$ , and strain rate,  $\dot{\epsilon}$ . The impact velocity ranges should be considered only as reference points. In fact, these transitions are extraordinarily flexible since deformation processes under impact loading depend on a long series of parameters in addition to impact velocity.

Table 1. Impact response of Materials



A complete treatment of the impact response of materials and structures would demand that account be taken of the geometry of interacting bodies, elastic-plastic and shock wave propagation, hydrodynamic flow, finite strains and deflections, strain rate effects, work hardening, thermal and frictional effects, and the initiation and propagation of failure in the colliding materials. An analytical approach would not only be formidable but would also require a degree of material characterization under high strain rate loading that could not be attained in practice. Hence, much of the work in this field has been experimental in nature. Existing analytical models generally incorporate a high degree of empiricism and focus on one or two aspects of the impact response of solids. Extensive reviews of existing models have appeared recently [2,3]. This paper focuses on numerical techniques for high velocity impact (0.5-2 km/s) simulations, their current capabilities and limitations. Some remarks about anticipated developments are also made. For the sake of completeness, the basic mechanisms involved in the penetration and perforation of solids are stated. Emphasis is placed on solid-solid impacts where both loading and response times are in the sub-millisecond regime. No account is given of the impact response of composite materials. Problems dealing with blast loading or shaped charge attack of structures are beyond the scope of this paper.

## 1. Penetration and Perforation of Solids

Penetration may be defined as the entrance of a projectile into a target without completing its passage through the body [2]. This involves either embedment or rebound of the striker and the formation of a crater in the target. Perforation, on the other hand, implies the complete piercing of a target by the projectile. Such processes occur in a time frame of several to several hundred microseconds. Targets and projectiles are deformed severely during such encounters.

Consider the events which occur in projectile and target during impact. For purposes of this discussion, consider the projectile to be in the form of a long rod, generally cylindrical in shape, with conical, ogival, hemispherical or flat nose. When such a projectile strikes a target, strong compressive waves propagate into both bodies. If the impact velocity is sufficiently high, relief waves will propagate inward from the lateral free surfaces of the rod and cross at the centerline, creating a region with high tensile stress. This tensile region can cause fracture in sufficiently brittle materials such as high strength steels. This effect will be enhanced if centerline porosity or other imperfections exist in the projectile material. For normal impacts, the state of stress is clearly two-dimensional. For oblique incidence, there is the additional complication of bending stresses due to the asymmetry of the loading. Under the proper combinations of projectile geometry, material characteristics and impact velocity, the combined bending and tensile stresses can lead to projectile failure and ricochet.

The initial compression wave in the target is followed quickly by a release wave. When the initial compressive wave reaches a free boundary in the target, an additional release wave is generated. If the combination of load intensity (tensile) and duration exceeds a critical value for the target material, failure will be initiated.

Targets are best classified following the definitions in [2]. A target is said to be:

- a. semi-infinite if there is no influence of the distal boundary on the penetration process
- b. thick if there is influence of the distal boundary only after substantial travel of the projectile into the targets
- c. intermediate if the rear surface exerts considerable influence on the deformation process during nearly all of the penetrator motion
- d. thin if stress and deformation gradients throughout its thickness do not exist.

Impacted materials may fail in a variety of ways, the actual mechanism depending on such variables as material properties, impact velocity, projectile shape, method of target support, and relative dimensions of projectile and target. Figure 1, adapted from [2,4], shows some of the dominant modes for thin and intermediate thickness targets. Spalling, tensile failure due to the reflection of the initial compressive wave from the rear surface of a finite thickness plate, is a commonplace occurrence under explosive and intense impact loads, especially for materials stronger in compression than in tension. Scabbing is similar in appearance, but here fracture is produced by large deformations and its surface is determined by local inhomogeneities and anisotropies. Fracture due to an initial stress wave exceeding a material's ultimate strength can occur in weak, low-density targets while radial cracking is common in materials such as ceramics where the tensile strength is considerably lower than the compressive strength.

Plugging failure has been studied extensively, both analytically and experimentally. Impact by a blunt or hemispherically-nosed striker on a finite thickness target at a velocity close to the ballistic limit (the minimum velocity required for perforation) results in the formation of a nearly cylindrical slug of approximately the same diameter as the striker which is set in motion by the projectile. The mechanism for plug formation has been termed "adiabatic shear banding" because of the hard white bands with sharp boundaries observed by etching sections of plates after plugging failure [5]. The generally accepted mechanism leading to plugging failure envisions occurrence of a plastic shear instability at the site of a stress concentration in an otherwise uniformly straining solid. The work of plastic deformation is converted almost entirely into heat which, because of the high deformation rates, is unable to propagate a significant distance away from the plastic

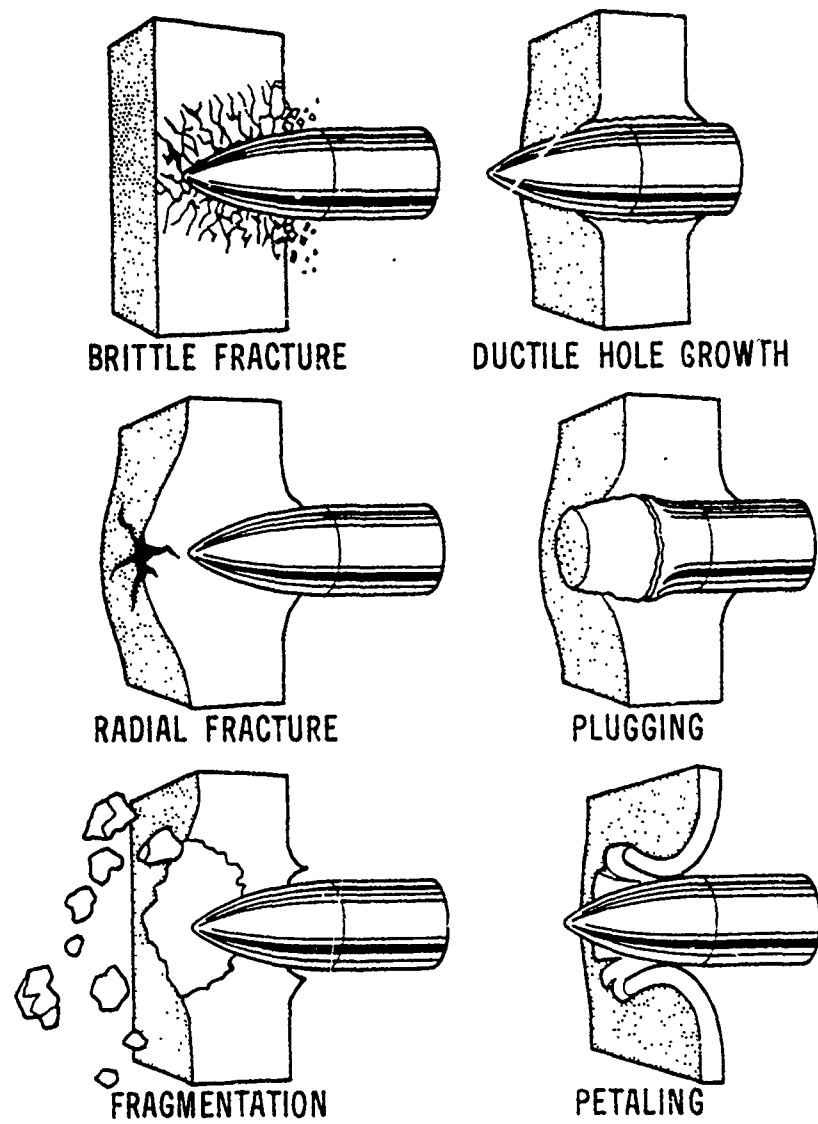


Figure 1. Failure modes in impacted plates

zone. As a result, the temperature in the zone rises, encouraging additional local plastic flow and concentrating the local plastic strain still further. The process continues and results in the propagation of a narrow band of intense plastic strain through the material along planes of maximum shear stress or minimum strength until unloading occurs or the material fractures. For striking velocities exceeding the minimum perforation velocity by more than 5-10%, multiple fragments rather than an intact plug will result. Plugging failure is quite sensitive to the impact angle and nose shape of the projectile.

Petalling is produced by high radial and circumferential tensile stresses after passage of the initial stress wave. The high stress fields occur near the tip of the projectile. Bending moments created by the forward motion of the plate material pushed by the striker cause the characteristic deformation pattern. It is most frequently observed in thin plates struck by ogival or conical bullets at relatively low impact velocities or by blunt projectiles near the ballistic limit. Petalling is accompanied by large plastic flows and permanent flexure. Eventually, the tensile strength of the plate material is reached and a star-shaped crack develops around the tip of the projectile. The sectors so formed are then pushed back by the continuing motion of the projectile forming petals.

For thick targets impacted by malleable materials at velocities exceeding 1 km/s, there is a hydrodynamic erosion and inversion of the penetrator material against the receding face of the penetration channel in the target. The target material is forced aside much as though a punch were being pushed into it, although the channel is much bigger than the penetrator diameter.

A combination of ductile failure and spalling seems to be characteristic for the failure of thick plates of low or medium hardness.

Material failure under impact loading is a most complex process. Even though one of the failure models depicted in Figure 1 may dominate, a second or third mode frequently accompanies the principal failure mode to a lesser extent.

In view of the complexity of penetration processes, it is not surprising that the bulk of the work in this area is experimental in nature. Terminal ballistic test techniques, aside from routine proof tests, vary mainly in the degree of instrumentation provided and hence the amount of data retrieved.

The most common type of ballistic test is designed to obtain information about

- a. the velocity and trajectory of the projectile prior to impact
- b. changes in configuration of projectile and target due to impact
- c. masses, velocities, and trajectories of fragments generated by the impact process.

Projectile trajectories may be determined in a number of ways; high-speed photography, orthogonal flash radiography or from yaw card measurements. Yaw cards are thin paper or plastic sheets located along the anticipated trajectory. Interaction of the projectile with the yaw cards does not generally affect its motion. The position of the perforations on the yaw cards determines projectile location in the plane perpendicular to the trajectory. The shape of the perforation allows flight orientation to be determined.

The striking velocity is determined from a measurement of transit times over fixed distances. The time of arrival at predetermined locations is established by the closing or opening of electrical circuits, interruption of light beams, synchronized photography or flash radiography of the projectile.

An example of a test setup for retrieval of penetration data for solid (kinetic energy) projectiles is shown in Figure 2. It is a

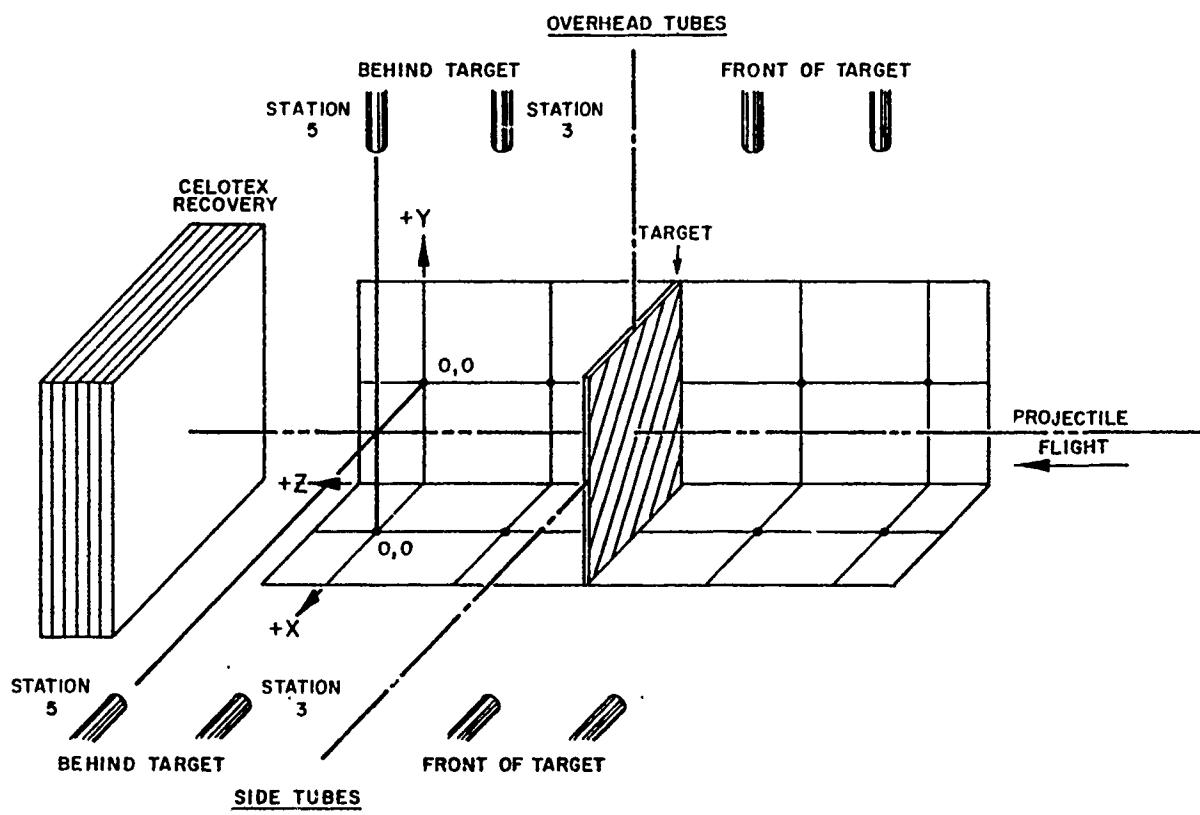


Figure 2. Experimental test set-up of x-ray instrumentation for obtaining penetration data for projectiles

typical arrangement used for small scale (65 gram or less) penetrators at the US Army Ballistic Research Laboratory [6] and sufficiently flexible so that changes (such as the addition of x-ray tubes or high-speed framing cameras) can be made to accommodate a variety of test requirements and projectile types. The x-ray system consists of orthogonal pairs of x-ray tubes (105 or 150 kv) arranged as shown. A time delay generator in the system pulses each tube or set of tubes at preset intervals.

Four tubes, arranged in pairs, provide simultaneous orthogonal radiographs of the projectile in free flight before target impact. The projectile striking velocity and orientation are measured from these radiographs.

A similar tube arrangement behind the target provides orthogonal radiographs to supply the data needed to determine the residual parameters. Additional tubes are usually added to view the projectile impacting and penetrating the target. Details of testing and data acquisition methods are given in [7-8].

In situations where fragment spray must be characterized for use in vulnerability analyses, recovery of fragments by procedures that inflict minimal damage to the fragments is necessary. The most common recovery media are stacks of plywood or cane fiber board, although other methods have been considered [9]. If there are many fragments, the task of measuring individual fragment masses, speeds, and directions of travel from multiply-exposed x-ray films and their correlation with recovered fragments is formidable due to problems of identifying individual fragments on the orthogonal film pairs. Procedures for fragment data acquisition, reduction and reporting are in [10-11]. Examples of typical small-scale terminal ballistics results are to be found in [12].

Post-mortem measurements on projectile and target include determination of the principal dimensions of the target crater such as depth, diameter, and crater volume (or entrance and exit diameters for a perforation) as well as the final length, diameter, and mass of the projectile and other massive fragments. Procedures for making the measurements are given in [8].

In summary, then, the data extracted from conventional ballistic tests consists of the following:

- a. speed and orientation of the projectile prior to impact
- b. speed and orientation of major projectile pieces after perforation
- c. speed, mass, and spatial distributions of fragments behind the target
- d. hole size and mass loss in the target.

For advanced analytical and numerical techniques, such meager data is insufficient to permit unambiguous establishment of the principal mechanisms which were active during the impact process. Advances in instrumentation techniques now permit the above data to be supplemented with additional information. Recent developments in cineradiography and high-speed photography [13-16] permit determination of time histories of material motion during the penetration process. Instrumented impact tests [17-20] provide information about surface strains in projectiles and stresses in targets during the penetration process, information which is invaluable in validating numerical simulation methods for penetration problems [20].

The PHERMEX facility [21] at Los Alamos Scientific Laboratory provides another invaluable method for the study of penetration phenomena. Essentially a 6 MEV x-ray source, it is capable of generating extremely short duration pulses which can literally penetrate, or "see into" some 20cm of steel, thus providing radiographs of projectile behavior within the target. Reference [3] shows comparison of two- and three-dimensional computational results with radiographs obtained at the PHERMEX facility.

Impact testing can be done routinely and cheaply in small scale (projectile weights <100g) with the techniques described above. Cost of testing, including materials and fabrication costs, range from \$800-2000 per test depending on the amount of instrumentation and data reduction required. Costs for full-scale testing (3-4kg projectiles) are 5-10 times as much. Usually, a large number of data points are required to obtain statistically meaningful results. Partially to offset the high cost of testing and to supplement the information obtained from experiments, recourse is made to analytical techniques.

Analytical approaches have tended to fall into three categories:

a. empirical or quasi-analytical: algebraic equations are formulated based on correlation with a large number of experimental data points and these are used to make predictions to guide further experiments. Such efforts are usually closely related to tests performed to discriminate between the performance characteristics of various materials or structures for a particular design objective. In general, these efforts do not significantly advance our understanding of material behavior and processes and will not be considered in this paper. A variety of such models for penetration and ricochet have been reviewed by Recht [22]. Similarity modeling for penetration mechanics is discussed in a chapter of the book by Baker et al [23].

b. approximate analytical methods: these concentrate on one aspect of the problem (such as plugging, petalling, spall, crater formation, etc.) by introducing simplifying assumptions into the governing equations of continuum physics in order to reduce these to one- or two-dimensional algebraic or differential equations. Their solution is then attempted, frequently in the course of which additional simplifications are introduced. With few exceptions, such analyses tend to treat either the striker or the target as rigid and rely on momentum or energy balance, or both. Only a few papers are concerned with predicting the deformation of both projectile and target. Furthermore, almost all such analyses either require some empirical input or rely on material parameters not readily available or measurable.

c. numerical methods: for a complete solution of impact problems, one must rely on a numerical evaluation of the governing equations of continuum physics. Finite difference and finite element methods are capable of attacking the entire set of field equations, have greater flexibility than various algebraic equations and can accurately model transient phenomena. They are still approximate in nature (one solves a set of discretized equations rather than the corresponding differential equations) but at present, errors associated with material properties are usually far greater than errors inherent in the numerical methods. Current interest centers on three-dimensional computational schemes for wave propagation and impact studies.

While the computational approach does offer the advantages of a complete treatment of the impact problem, with exact representation of geometries involved and without recourse to simplifying assumptions, it is not without its drawbacks. The price of complexity in analytical models is an ever-increasing need for additional information about dynamic material behavior. Advanced computational methods require fairly detailed information about the behavior of materials at high loading rates, especially their failure under such loading. This is information which is only now becoming available. Hence, computer codes are only as good as the material descriptions contained therein. Table 2 compares some of the advantages and disadvantages of three-dimensional computer codes and full-scale experiments. These issues are discussed more fully in the following sections and in [3]. In general, neither the experimental nor the analytical approach alone is effective in solving impact problems. The best results come from a judicious combination of both.

Table 2. Computations Versus Experiments

Constraints	Computer Simulation	Field Experiments
Cost	Typical 3D simulation costs ~\$1000 for ricochet situations, ~\$6000 for penetration simulation.	Typical cost for one shot is \$7500 (including materials and fabrication costs and data reduction).
Time	Up to one week may be needed to grid and debug problem, several weeks to obtain and analyze results.	Once materials have been fabricated, one to two shots per day can be obtained.
Information	Maximal output - displacements, stress, strain, strain rate, momenta, energies, forces, and moments.	Minimal - initial and final velocity and orientation for projectile; residual projectile mass; target hole size and mass loss.
Unknowns	Results depend on material model, material properties, failure model.	Uncertainties in material properties, initial conditions and boundary conditions manifested as data scatter.
Utility	Excellent base for construction of approximate analytical models for parametric studies.	Time and cost constraints almost never permit acquisition of data base with enough variation of parameters to construct unambiguous models.

## II. NUMERICAL SIMULATION OF IMPACT PHENOMENA

### A. General Considerations

Analytical models, although limited in scope, are quite useful for developing an appreciation for the dominant physical phenomena occurring in a given impact situation and for sorting experimental data. They may even be useful in making predictions, provided care is taken not to violate the simplifying assumptions introduced in their derivation or exceed the data base from which their empirical constants are derived. If a complete solution to impact situations is necessary, recourse must be made to numerical simulation. This is especially true for oblique impacts or situations where a three-dimensional stress state is dominant for there are virtually no models which can deal with such complexity. Two- and three-dimensional computer codes obviate the need for various simplifications and are capable of treating complex geometries and loading states. However, their accuracy and utility is limited by the material descriptions embodied in their constitutive equations. Excellent results have been obtained for situations where material behavior is well understood and characterized, eg, [ 24].

Numerical simulations of high velocity impact phenomena in two dimensions have been performed routinely for a number of years. Current interest centers on three-dimensional simulations. The range of problems addressed is fairly wide, including computations in the hypervelocity regime in order to determine structural configurations capable of protecting spacecraft against meteorite impact and study of the erosion and fracture of missile and space vehicle heat shields during re-entry. The bulk of the effort has been on military problems, namely the penetration and perforation of solids and structures subjected to kinetic energy (inert) missile and shaped charge attack as well as the reverse problem of the design of armors against such threats. In geophysics, computations complement the study of materials under very high pressures and provide historical details for formation of craters produced by meteor impact, eg, [25]. Industrial problems addressable computationally include explosive forming, explosive welding, shock synthesis of materials, mining, and massive earth removal.

A compact description of the computational process is shown in Figure 3. The three stages listed may be incorporated in a single computer program, or code, or may exist as three distinct codes. At any rate, some sort of automatic generation capability exists to provide a detailed computational mesh for the geometry of interest from an abbreviated description provided by the user. This information is coupled to a description of the materials making up the geometric bodies by specifying appropriate parameters for the equation of state, the stress-strain relationship used by the code in both the elastic and plastic regimes, and the failure criteria to be used. A description of boundary and initial conditions ends this stage of the process. The pre-processor, as this stage is commonly called, prepares the information in a form usable by the next part, the main processor, and also prints or interactively displays the initial geometry and conditions for user verification. The current crop of codes (those developed within the last few years) tend to allow the user, via a graphics terminal, to view the results, either complete or partial, of the pre-processor and modify the computational grid, initial conditions, boundary conditions, and material description.

The conservation laws for mass, momentum and energy, coupled to an equation of state for determination of pressures, a constitutive relationship, a failure criterion and a post-failure model are cast into finite difference or finite element form and integrated in time in the next phase, or main processor, using the information generated by the pre-processor. These computations are of necessity quite long and demanding of computer storage and except for a very few problems never run to completion in one pass. Hence, provision is almost always made for a restart capability, so that computations may be resumed after interruption for physical or administrative reasons.

## PRE- PROCESSOR

## MAIN PROGRAM

## POST- PROCESSOR

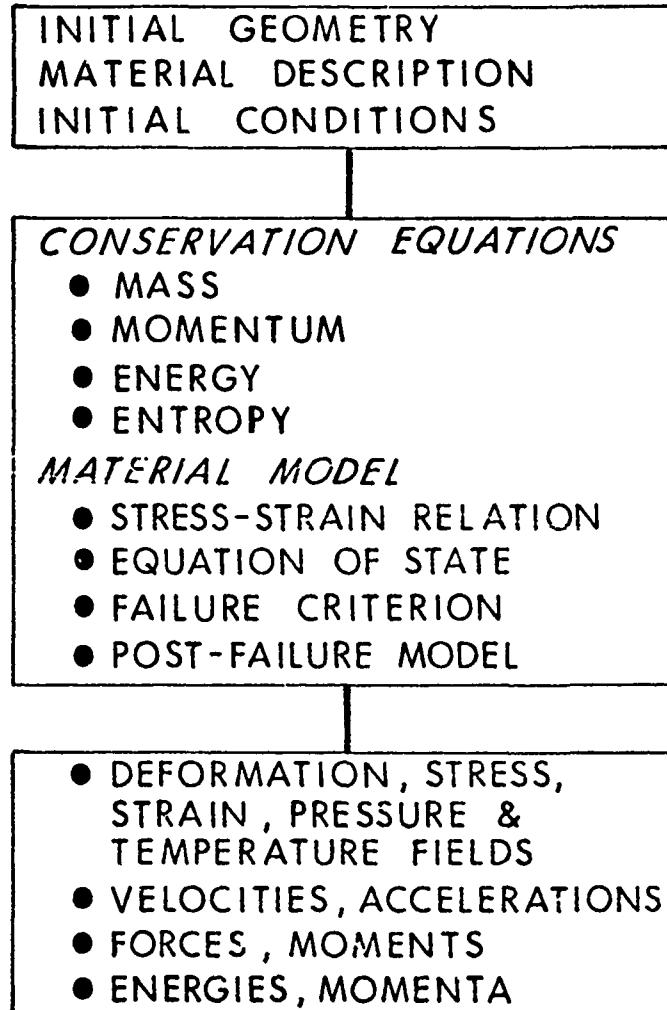


Figure 3. Computational process for impact simulation

Results of the computations, or output, is generally massive. Codes typically produce full-field descriptions of physical quantities and material conditions (intact, failed, plastically deformed) throughout the problem as a function of time. Output listings of two- and three-dimensional codes can run into hundreds of pages and are impossible to read (indeed, sometimes to carry). Recourse is therefore made to post-processors, computer programs which prepare graphical displays of the items of interest, ie, deformation, velocity, temperature, energy fields at given times, and time histories of variables of interest, etc. The degree of sophistication of these plot packages varies considerably from code to code. They are also very dependent not only on the machine on which the code is installed but also on the installation. Transferring both code and plot package from one installation to another can be a nontrivial task. It is not unusual for such transfers to require several man-months of full-time effort.

The decision to use such codes should not be made lightly for in no sense can the current crop of programs be treated as "black boxes"! As a rule, at least three to six months effort is required before new users can run practical problems on existing codes. During the learning period, frequent contact with the code developers or persons experienced in their use will be required. Even after the essentials have been mastered, pathological situations will arise which will require guidance from experienced users and may require code modification. Aside from the man-months expended, computational costs will be non-negligible. However, the judicious combination of computer simulations and experiments (which will be accompanied by efforts to characterize candidate materials at high strain rates if such data is not already available) can lead to considerable improvements in engineering design with reduced manpower and computer costs.

Some examples of results which can be achieved with current computer codes are presented further on. Throughout the following, it should be kept in mind that computational results are directly related to the quality of the material model in the code-the better the description of material behavior at the strain rates encountered experimentally and of its failure modes at those strain rates, the better the computational results. Improper materials characterization leads not only to quantitatively incorrect results but frequently to descriptions which are qualitatively incorrect. Imperfect understanding of this situation has frequently led to "...an undesirable iterative procedure of matching imperfectly understood experiments with theoretical computations based on incomplete models" [26]. Fortunately, this is an area of intense activity currently so that it is not unreasonable to expect that within the next few years improved understanding of the dynamic behavior of materials at ultra-high loading rates will lead to improvement in code quantitative predictions.

After a brief look at various aspects of the numerical simulation of the dynamic behavior of impacting continuous bodies, specific characteristics of two- and three-dimensional codes will be mentioned. One-dimensional codes and results will not be considered. For these, the reader will be referred to an extensive literature. The primary emphasis will be on three-dimensional methods for analysis of impacting solids and results.

### B. Discretization Methods

It is necessary in a computer analysis to replace a continuous physical system by a discretized system. In the discretization process, the continuum is replaced by a computational mesh. The discretization techniques most commonly used are the finite difference and finite element methods.

Historically, the finite difference codes came first as programs were developed to treat hypervelocity impact situations. Later a material strength model, usually a simple elastic-perfectly plastic or rigid plastic model, was tacked on to the codes to treat the later stages of hypervelocity situations or penetration problems in the ordnance velocity regime. Finite element methods began at the opposite end of the loading rate spectrum, being originally used to approximate the behavior of arbitrary structures and structural systems subjected to static loadings. Recently, finite element programs capable of treating problems in wave propagation, large plastic flow, and fluid flow have appeared and are taking their place with the finite difference codes.

In the finite difference method, spatial and time grids are constructed by replacing derivatives in the governing equations of continuum dynamics with difference approximations. Standard techniques for solution of large equation sets are employed to obtain spatial solutions. Solutions in time are obtained by integration.

The finite element approach is an outgrowth of structural analysis techniques. Here, instead of manipulating the governing equations into differential equation form and then attempting a numerical solution, the discretization procedure is employed from the very start. The procedure [27] consists of:

- a. dividing the continuum by means of imaginary lines into a finite number of regions, or elements, which are assumed to interact only at a discrete number of points called nodes. The displacements at these nodal points are the basic unknowns of the problem.
- b. a set of functions is postulated to define displacements at any point within an element in terms of the nodal displacement.

c. these displacement functions now define a state of strain within each element. These, together with constitutive properties, then define the state of stress.

d. a system of forces concentrated at the nodes which equilibrate external loads is determined. This procedure results in a stiffness relationship-equations relating internal loads, external loads, and nodal displacements. Individual element (local) data are then assembled into global arrays and solutions for nodal displacements are obtained with conventional techniques for large systems of algebraic equations. Element strains and stresses are then determined from the nodal displacements.

As the above descriptions imply, a common property of both methods is the local separation of the spatial dependence from the time dependence of the dependent variable. This allows separate treatment of the space and time grids. Time integration methods will be mentioned shortly. Characteristics of the spatial discretization schemes are discussed in several papers [28-35]. The following is therefore a brief summary of their principal conclusions.

It has been shown [28] that the discrete forms of the equations of motion of the finite element method are equivalent to those of the finite difference method for a number of cases. Thus, since there is no basic mathematical difference between the two methods they should have the same degree of accuracy in numerical computations. The main differences lie not in the methods themselves but in the data management structure of the computer programs which implement them.

Finite element codes have a distinct advantage in treating irregular geometries and variations in mesh size and type. This is because in the finite element method, the equations of motion are formulated through nodal forces for each element and do not depend on the shape of the neighboring mesh. In the finite difference method, equations of motion are expressed directly in terms of the pressure gradients of the neighboring meshes. This is not inherently a problem, but the difference equations must be formulated separately for irregular regions and boundaries.

Another major difference occurs in numbering of meshes. In finite difference programs, the regularity of the mesh implicitly establishes the connectivity information. In finite element programs, mesh connectivity is explicitly stored, a feature which facilitates automatic generation of complex mesh systems. This limitation can be overcome for finite difference codes, but versatility is generally achieved at the expense of large computer storage and CPU time.

### C. Mesh Descriptions

The bulk of the computer codes for impact studies fall into two categories: Lagrangian and Eulerian. Lagrangian codes follow the motion of fixed elements of mass with the computational grid being fixed and distorting with the material. Lagrangian methods have several advantages:

a. the codes are conceptually straightforward since the equations of mass, momentum, and energy conservation are simpler due to the lack of convective terms to represent mass flow in the coordinate frame. Since fewer computations are required per cycle, they should be in theory computationally faster. However, see below.

b. material interfaces and free surfaces are stationary in the material coordinate frame, hence allowing sharp definition and straightforward treatment of boundary conditions. It should be noted though that fairly complex logic is required to define behavior at material interfaces, ie, opening and closing of voids, frictional effects. While such logic enhances the generality and applicability of the codes, a price is paid in the number of additional computations required per cycle, thus slowing overall run time.

c. some constitutive equations require time histories of material behavior. In the Lagrangian method, this is easily and accurately accounted for.

A typical example of a Lagrangian grid is shown in Figure 4. As already mentioned, the Lagrangian computational grid distorts with the material. Inaccuracies in the numerical approximations grow when cells become significantly distorted due to shear or fold over themselves resulting in negative masses. These problems can be overcome to some extent through the use of sliding interfaces and rezoning.

Grid distortions can be reduced in some problems by use of sliding interfaces either between different materials which can be expected to slide over one another as the motion proceeds or in regions where very large shears and fractures can be expected to develop. Most sliding interface methods are based on the decomposition of acceleration and velocity into components normal and tangential to the interface. Motions in the normal direction are continuous when materials are in contact but are independent when they are separated. Tangential motions are independent when materials are separated or the interface is frictionless, but are modified if there is contact and a finite frictional force is present. On sliding interfaces, frictional forces ranging between zero and infinity may be specified. Materials at either side of an interface may separate if a specified criterion is exceeded and may collide again if previously separated.

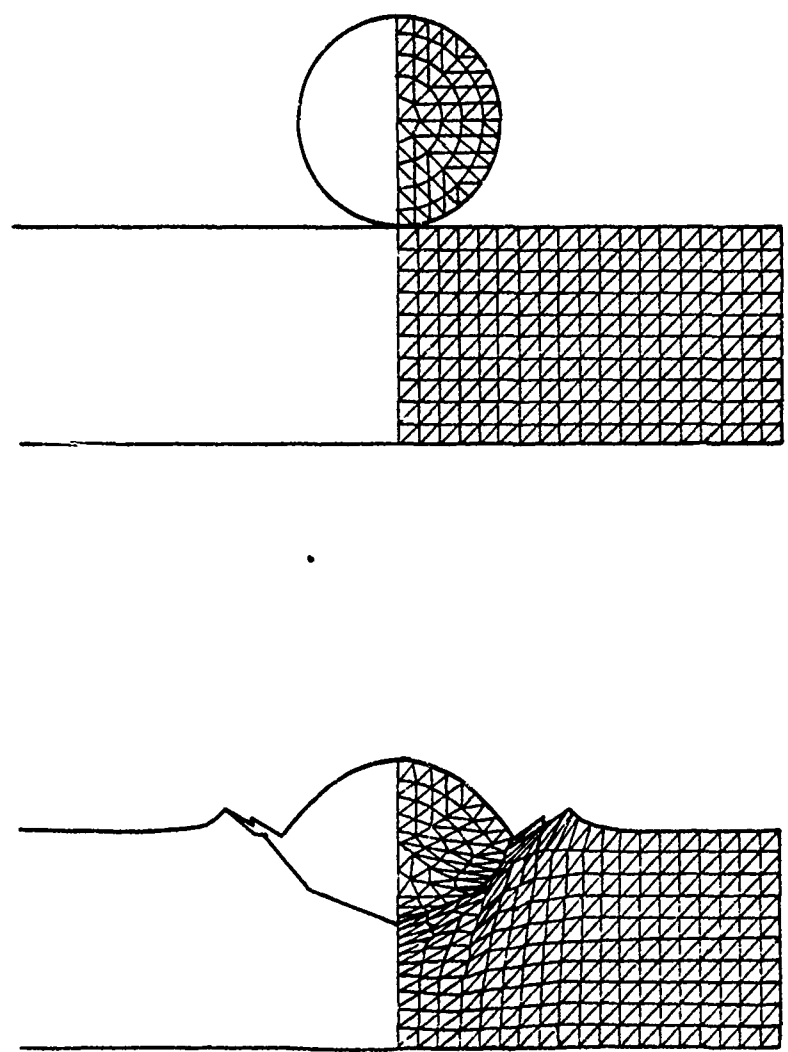


Figure 4. Lagrangian computational grid

When severe grid distortions cause errors in the discretization scheme to become very large and the allowable time step to become very small, recourse must be made to rezoning. A new grid is overlaid on the old one and the rezone program maps mesh quantities of the old grid onto the new grid such that conservation of mass, momentum, and total energy and the constitutive relationship are satisfied. Rezone techniques have been used quite successfully in one-dimensional codes, especially to increase definition in regions where physical quantities vary rapidly. For two- and three-dimensional codes, however, rezoning is a costly and complex operation. Difficulties arise in averaging internal state variables representing material memory, since a given new mesh may cover several old meshes each of which has experienced a somewhat different history. Several rezoning operations may be required before a successfully rezoned grid is obtained and the final result is very much a function of the experience of the operator performing the rezoning. Even the most complicated and sophisticated rezone routines have been disappointing for the two-dimensional case, with the apparent exception of the TOODY code.

In the Eulerian approach, the computational grid is assumed fixed in space while the continuum passes through it (Figure 5). Material can be represented as either discrete points or as a continuum. Such codes are ideally suited for large distortion problems but unless Lagrangian features are incorporated, free surface motions and material interface conditions are not accurately computed due to diffusion. Without Lagrangian features, it is not possible to obtain material time histories. Eulerian codes are absolutely required if mixing of materials initially segregated is important.

Since no one computational technique can handle all situations in impact dynamics, hybrid methods have been developed. Many variations exist. The most common techniques include use of Lagrangian tracer particles in Eulerian codes to accurately treat material interfaces or use of an Eulerian method at the beginning of a computation when gross flow and distortions are expected, then mapping to a Lagrangian grid for completion of the calculations. Alternative approaches include mixed Eulerian and Lagrangian computations in parallel. Convected coordinate and hybrid methods have also been used. These are discussed in an excellent review article by Herrmann [32].

#### D. Temporal Integration Schemes

Integration of the discretized equations of continuum mechanics can be accomplished in a number of ways [28-29, 31, 36]. Commonly, the central and forward difference schemes are employed. The methods are called explicit if the displacements at some time  $t+\Delta t$  are independent of the accelerations at that time. The computational flow is quite straightforward. At any time step, the velocities and displacements are known. The rate of deformation or the strain can be computed from the strain-displacement relations and the stresses at that time

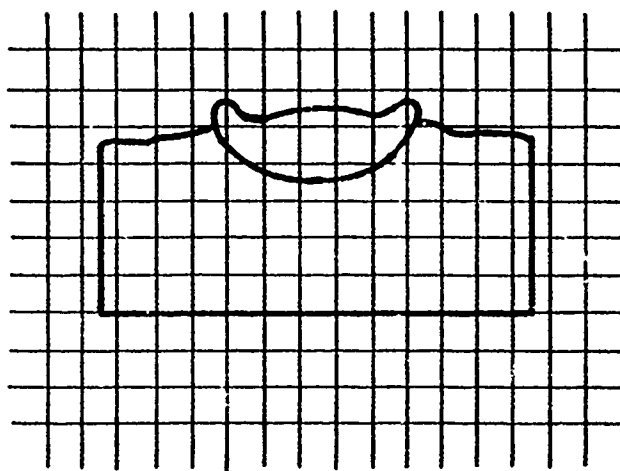
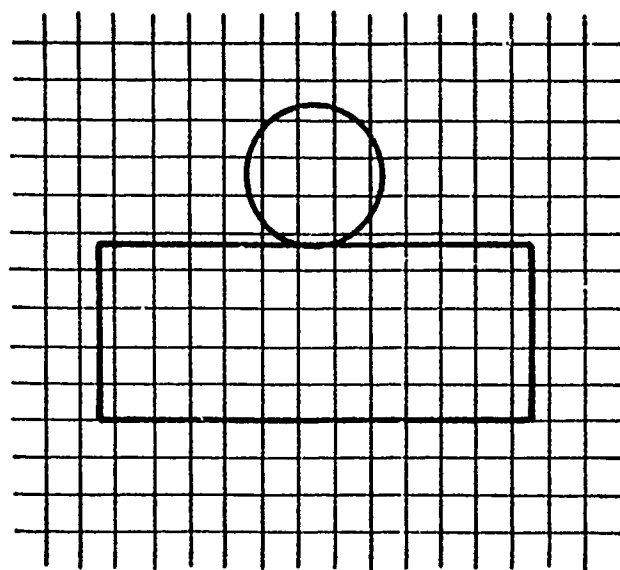


Figure 5. Eulerian computational grid

step are found from the constitutive relationship. The equation of motion is then used to find the accelerations which, together with velocities, are stepped forward in time to find new displacements and the entire procedure is repeated once again.

The computed response may become unstable (grow without bound) in explicit integrations unless care is taken to restrict the size of the time step. This problem has been studied rigorously for linear problems by Courant, Friedricks, and Levy [37] who found that in explicit integration the computation will be stable if the time step  $\Delta t$  satisfies the relation

$$\Delta t \leq 2/\lambda \quad (1)$$

where  $\lambda$  is the highest natural frequency of the mesh. No rigorous stability criterion has been determined for nonlinear problems but it is customary to determine the time step from

$$\Delta t = \frac{k\lambda}{c} \quad (2)$$

where  $\lambda$  is the minimum mesh dimension in the computational grid,  $c$  the sonic velocity, and  $k$  a factor chosen to be less than unity, generally between (0.6- 0.8).

Problems involving impact at ordnance velocities (0.5-2 km/s) result in a strong initial shock wave (alternatively, a large stress or velocity gradient) which can lead to material failure and must be accurately resolved. This demands fine spatial as well as temporal resolution and results in very small time steps and a large number of computational cycles.

Typically, for design problems, computations must be run to tens or hundreds of wave transit times across the characteristic length dimension of the problem. This places a severe burden on computer resources and has spurred investigation of implicit integration schemes.

In an implicit scheme, the displacements at any time  $t+\Delta t$  cannot be obtained without a knowledge of the accelerations at the same time. The relationships between velocity, displacement, and accelerations must be combined with the equations of motion and the resulting set of simultaneous equations solved for the displacements. The resulting nonlinear equations are generally solved by some kind of linearization method. Predictor-corrector schemes or trapezoidal techniques such as the Houbolt method, as well as the Wilson  $\theta$  method and the Newmark  $\beta$  method are popular [29, 35].

Most implicit methods have been shown to be unconditionally stable. However, the price of stability is the need to solve a set of equations at each time step. The local truncation error of most implicit and explicit schemes is of order  $(\Delta t)^3$ . While this is insignificant for explicit schemes, it is a matter of concern for implicit methods where the time step is so much larger.

In general, it has been found [30, 31, 36] that for wave propagation methods, the time step for implicit methods must be about the same as that for explicit methods in order to satisfy accuracy requirements. Since implicit methods require considerably more computations per cycle than explicit integrations, their use has generally been limited to problems where the details of wave propagation are not as significant as the overall response of the material.

#### E. Computer Resource Requirements

Questions of accuracy and resolution required for dynamic stress wave solutions are discussed in [36]. Such solutions are characterized by a very high frequency content and adequate numerical representation requires a large number of meshes in areas where large stress gradients propagate. Two-dimensional computations are routinely done with 4,000-10,000 meshes or elements. Adequate resolution in three-dimensional problems is even more difficult to achieve. For practical problems 20,000-50,000 meshes are not uncommon. For high velocity impact situations, adequate information for design purposes (projectile velocity and orientation, extent of deformation in projectile and target, energy deposition in the target) may be obtained with 20-25,000 meshes. Excellent correlation with experiment was obtained for an oblique impact situation with 25,000 elements [3] while the same calculation with 12,000 elements underpredicted penetration depth by 40%. For problems involving steep gradients or advanced failure models, even greater resolution may be required. Since most practical problems are run with variable meshes to conserve CPU time and computer storage, there is no a priori method for determining an optimum grid for a given computation, although guidelines for educated guesses exist [30, 36]. Experienced code users can generally arrive at acceptable grids within a few iterations.

Computing costs tend to be quite high for production problems. Running times for one-dimensional codes are measured in minutes. For two-dimensional codes with some 5-6000 meshes or elements, running times of several hours on CDC 7600 class machines are typical. Three-dimensional problems will typically run from 4-10 hours or longer. Three-dimensional problems also place severe limitations on computer storage. It is virtually impossible to run a three dimensional impact problem totally in-core. Thus, to permit adequate resolution, most codes have provisions for keeping only a small portion of the grid in core and the remaining information on a mass memory device.

There is still an upper limit on resolution, though. If the number of meshes or elements is too great, the bulk of the total computer time will be spent in data transfer and very little in advancing computations.

As expensive as such calculations may be, they are often less costly than full-scale experiments. Indeed, in certain situations, experimentation may not be possible and reliance must be made on computations. Additionally, unless the software is reasonably efficient in permitting automated mesh generation and graphical representation of results, the major portion of the total cost will be associated with manpower charges incurred by analysts performing numerical studies. An illuminating example is shown in [36].

#### F. Material Model

It is common in existing production codes for the study of high velocity impact phenomena to divide the deformation behavior of metals into volumetric and shear (deviatoric) parts. Metals undergo plastic yielding at modest levels of deviator flow stress. This is usually taken to be independent of pressure, so that the volumetric behavior can be treated independently of the shear behavior.

The volumetric behavior is described in terms of an equation of state relating pressure, volume and some thermal parameter, usually the internal energy or temperature. The Mie-Gruneisen equation of state is frequently used, although some codes allow a choice of equations. In the newer, modular, codes, equations of state can readily be changed.

For solid-solid impacts in the 0.5-2 km/s velocity regime, only moderate pressures (300-500 kb) are generated and these decay rapidly to values comparable to the strength of the material. Hence, the equation of state in impact calculations is of secondary importance. Considerable data exists for the current crop of equations in various compilations for most metals of interest [38-39] and additional data can readily be obtained. Consequently, the state of the art in equation of state is adequate for most present needs.

An incremental elastic-plastic formulation is used to describe the shear response of metals in present finite difference and finite element codes. The plasticity descriptions are usually based on an assumed decomposition of the velocity strain tensor,  $\dot{\epsilon}$ , into elastic and plastic parts

$$\underline{\dot{\epsilon}} = \dot{\epsilon}^e + \dot{\epsilon}^p \quad (3)$$

together with incompressibility of the plastic part

$$\epsilon_{11}^p + \epsilon_{22}^p + \epsilon_{33}^p = 0 \quad (4)$$

Stress and strain tensors are divided into volumetric and deviator parts. The volumetric parts, namely the pressure and volume, are determined through the equation of state. The von Mises yield criterion and the Prandtl-Reuss incremental theory are typically used to describe plastic behavior. Since strains in problems involving penetrations are large, questions have been raised regarding the validity of this approach and alternatives proposed [40-41].

Plasticity models for computations have been reviewed by Armen [42]. Generally, the plasticity models in wave propagation production codes are relatively simple elastic-perfectly plastic descriptions following the method formulated by Wilkins [43]. Minor modifications have been introduced to this basic description by allowing the yield stress to vary with the amount of plastic work, temperature, strain rate or some combination thereof, eg, [44].

Herrmann and Lawrence [45] have recently reviewed material models used to describe stress wave propagation in metals, polymers, composites and porous materials. They find that for metals a perfect plasticity approach can serve as a first order approximation for many high strength alloys used in impact situations in the ordnance velocity regime (0.5-2 km/s) provided care is taken to select an average dynamic value of flow stress. Excellent results have been obtained with this approach [24, 46-47] and it is appealing from the point of view that the degree of dynamic material characterization required is quite low. Also, many high strength alloys show little variation in flow stress with strain rate and relatively low rates of strain hardening.

A priori determination of an appropriate dynamic flow stress is another matter however. Until very recently such information was not generally available. In a few cases, a dynamic yield stress can be estimated from static test data but in general the understanding of micromechanical deformation mechanisms at very high strain rates is so limited that estimation of dynamic properties from static data is hazardous. This approach is best used in conjunction with dynamic material property tests.

No one dynamic property test technique can provide information over the range of stresses, strains, strain rates, and temperatures encountered in high velocity impact. Several relatively simple techniques exist however which, despite their limitations, provide useful data for numerical computations. Methods for dynamic characterization of materials have been reviewed by Lindholm [48]. Several methods commonly used from which a substantial body of data exists will next be briefly described.

The split Hopkinson bar consists of a striker bar, incident bar, transmitter bar, and associated instrumentation. The test specimen

is sandwiched between the incident and transmitter bar. Measurement of the elastic waves in the pressure bars which are reflected and transmitted by the specimen yield average stress, strain, and strain rate as functions of time in the specimen once the specimen has reached homogeneous deformation. This data can be manipulated to obtain a dynamic stress-strain curve for the specimen material. The technique can be employed in tension, torsion, and compression at strain rates from  $10^2$  to  $10^4$   $s^{-1}$  [48-53].

Care must be taken in performing split-Hopkinson bar tests that assumptions governing analysis of the data not be violated. The pressure bars and specimen are assumed to be in a state of uniaxial stress so that radial inertia effects are neglected. Care must also be taken in selecting specimen size and lubrication of specimen-bar interfaces to minimize end effects.

An alternate method involves the free-flight impact of identical bars [54-56] producing a well-defined constant velocity boundary condition and an accurate measurement of surface strain by optical techniques employing diffraction gratings ruled directly on the specimen. The technique was perfected by Professor James Bell of Johns Hopkins University. For each test, a record of surface strain and surface angle is made. From a series of such tests, Bell constructs a dynamic stress-strain curve by first establishing that the velocity of propagation of each increment of plastic strain is constant. This requires measurement of strain-time profiles at several axial positions along the length of the bar. If the average propagation velocities are indeed found to be constant it is a sufficient condition for the one-dimensional rate-independent theory of plasticity to hold [57] and permits determination of stress corresponding to a given strain to be obtained.

This technique also has a number of limitations which have been more fully discussed elsewhere [48, 58]. Radial inertia effects near the end of the struck specimen are unavoidable and confuse interpretation of measurements.

Another technique, originally used by Taylor [59] and Whiffen [60], consists of firing a short cylindrical bar against a rigid surface. The struck end of the bar is subjected to large plastic strains and complex stress states. However, a simple analysis [59], later refined by Hawkyard [61], permits determination of an average dynamic yield stress in terms of the impact velocity and the residual length of the bar. Wilkins and Guinan [46] have examined the method in detail using the two-dimensional HEMP code. They find that overall agreement with experimentally determined deformation profiles can be determined with the dynamic average flow stress so obtained and that the flow stress for a number of materials was invariant over a limited range of strain rates.

If information at higher strain rates is needed, recourse must be made to plate impact experiments. Impact of a flat projectile on a flat target plate produces plane stress waves in which, because of symmetry, the strain is one-dimensional until reflections arrive from the plate edges. Strain rates from about  $10^4$ - $10^6$  s<sup>-1</sup> can be studied with this technique. Reviews have been given by Karnes [62] and Davison and Graham [63].

Provided care is taken to characterize materials at strain rates appropriate to problems being considered, excellent results can be obtained even with simple material models. The greatest limitation on the utility of computations for studying impact processes is in the modeling of material failure. Because of its importance, this topic will be treated separately. Next, a brief survey is given of the characteristics of currently popular two- and three-dimensional computer codes together with examples of their capabilities. One-dimensional codes and two-dimensional codes of historical interest will not be mentioned since these have already been extensively reviewed [26, 30-33, 64].

### III. CURRENT CODE CAPABILITIES

#### A. Two-dimensional Lagrangian Codes

The most prominent two-dimensional finite difference Lagrangian codes in use today are the HEMP code, developed by Wilkins of Lawrence Livermore Laboratories, and the TOODY/TOOREZ codes developed by Bertholf and his colleagues at Sandia Laboratories. Both codes employ a second order accurate finite difference representation first developed by Wilkins [42]. They are quite similar in essential features and capabilities. Both codes are well documented insofar as the fundamentals are concerned [65-69]. However, there are many versions of both codes running on a variety of machines. Potential users are therefore well advised to obtain not only the basic documentation but also to maintain close contacts with the users and systems people at the computer center from which their particular version is obtained. Many derivatives of HEMP exist, ie, the two-dimensional member of the PISCES family of codes marketed by Physics International through the CDC Cybernet network, CRAM and SHEP to name a few. The differences relate primarily to features required to implement the basic code on different machines and changes in pre- and post-processing capability.

The finite difference equations in the HEMP (Hydrodynamic, Elastic, Magneto & Plastic) code, employ a quadrilateral grid and may be solved in plane coordinates or with cylindrical symmetry. Slide lines are available which permit material motion with and without friction. Provision is also made for the opening and closing of voids. Boundaries may be fixed or free, stationary or moving. Both pressure and velocity

initial conditions may be specified. A mesh generation capability exists so that many geometric configurations may be generated with minimum user input. Alternatively, users may specify mesh configurations with a fair degree of detail manually.

The HEMP code runs on a variety of computers, though most users tend to prefer the CDC 6600 and 7600 machines. The precise configuration of the code and size of problems which can be run depend very much on the machine on which it is implemented.

The TOODY-TOOREZ codes are similar in the basics to HEMP. The finite difference equations in the TOODY code are discussed in some detail by Walsh [34]. Like HEMP, TOODY has been used successfully on a number of difficult practical problems. As with most production codes, instantaneous failure criteria based on maxima or minima of field variables were initially incorporated in the codes. Many users however have modified these and incorporated more sophisticated failure models to suit their particular needs.

The EPIC-2 (Elastic Plastic Impact Calculations in 2 Dimensions) code [70] is based on a Lagrangian finite element formulation wherein the equations of motion are integrated directly rather than through the traditional stiffness matrix approach. The code treats problems involving wave propagation and elastic-plastic flow. It is arranged to provide solutions for projectile-target impacts and explosive detonation problems. Material descriptions are incorporated which include the effects of strain hardening, strain rate effects, thermal softening, fracture, and spin. Geometry generators are included to permit quick generation of flat plates, spheres, and rods with blunt, rounded or conical nose shapes. Multiple slide lines (no frictional effects) are provided. A rudimentary post-processor provides plots of initial geometry, deformed geometry, effective stress, effective strain, pressure, and velocity fields. In addition, time-history plots of various system parameters (energies, momenta, penetration depth, etc.) may be obtained.

#### B. Two-dimensional Eulerian Codes

Two Eulerian codes currently popular for impact studies which incorporate all the desirable features of the Eulerian description of continuous material behavior while including features which enhance material interface and boundary definition are HELP and HULL.

The HELP code was developed by L. J. Hageman and J. M. Walsh. The current version [71] is a two-dimensional, multi-material first order finite difference code which has been used extensively to solve material flow problems in the hydrodynamic and elastic-plastic regimes. Although the code is basically Eulerian, material interfaces and free

surfaces are propagated in a Lagrangian manner through the calculational mesh as discrete interfaces across which material is not allowed to diffuse. The material model employed in HELP includes the Tillotson equation of state, modified to give a smooth transition between condensed and expanded states, a deviatoric constitutive relationship, a yield criterion defined to account for increase in strength at high pressures and decrease in strength at elevated temperatures, and failure criteria. Failure in tension is based on relative volume. When the relative volume in a cell reaches a certain value greater than a specified maximum distension, that cell is said to fail and computed tensions are zeroed out. A failure criterion based on maximum plastic work for modeling plugging failure is also available and has been used with reasonable success [72]. Recently, the Stanford Research Institute nucleation and growth model, NAG-FRAG, for ductile and brittle failure in metals has been incorporated in HELP [73]. However, it has not been tested on realistic problems.

The HELP code has been widely exercised and applied to a variety of problems in the ordnance velocity and hypervelocity regimes. Some interesting results are to be found in the paper by Sedgwick [74]. Good results are possible with HELP although considerable experience is required before the code can be used effectively. Its principal drawback is a lack of modularity which can turn simple modifications (ie, replacement of the equation of state) into major projects even for experienced users. In addition, because of the first order accuracy in the finite difference formulation, pathological problems are the rule rather than the exception for situations wherein material strength effects are dominant. A recent revision in the internal energy algorithm [75] should help somewhat. Good results can be expected for hypervelocity impact situations. Close association with the code developers in the early stages of implementation and use is mandatory for success.

The first version of the HULL finite difference code was written in 1971 by Matuska and Durrett at the Air Force Weapons Laboratory. In 1976, the code was rewritten to permit computation of elastic-plastic phenomena. The revision was quite extensive and the resulting code has improved the state of the art in Eulerian methodology. Computations with HULL can be performed for work hardening-thermal softening solids as well as high explosives, fluids, and gases. Lagrangian passive tracers are utilized in the code but for boundary definition HULL employs a diffusion limiting scheme. Combined with material preferential transport, the diffusion limiter provides sharp interface maintenance. In place of thermal equilibrium in mixed material zones, separate species energies are calculated. A rather novel material failure technique was added in 1977 by Matuska. When a metal is considered to have failed, a small but numerically significant quantity of void is inserted in the zone. The void is allowed to grow in size in subsequent cycles until the state of the real material in the zone no longer exceeds the failure

criterion. The void can completely take over a zone or neighboring zones if the physical situation decrees such growth necessary, ie, spall. Zone recompression can reduce the size of voids or eliminate them altogether. Excellent results with HULL have been obtained at the Air Force Armament Laboratory, Eglin AFB on formidable practical problems involving penetration of thick targets and target arrays. The HULL code runs on CDC 6600 and 7600 computers as well as Honeywell and IBM machines and has considerable flexibility in input preparation and displays of results. Documentation, however, is spartan [76-77]. Assistance from experienced users or code developers is virtually mandatory until additional documentation becomes available.

Other Eulerian codes used frequently for impact situations are DORF [78-79] which is quite similar to HELP in capabilities and problems and also CSQ [80-81] which is frequently used in conjunction with the TOODY code to guide rezoning operations. Typical results are to be found in [82].

### C. Three-dimensional Codes

A number of three-dimensional codes are available. With exceptions to be noted below, they are based on their two-dimensional predecessors, the general features of which are described above and in review articles [26, 32, 64].

The Lagrangian finite difference code HEMP3D [83] is an outgrowth of the two-dimensional HEMP code and is designed to solve problems in solid mechanics involving dynamic plasticity and time-dependent material behavior. It is based on an incremental formulation for elasto-plastic behavior, employs the von Mises yield criterion and relies on artificial viscosity for diffusion of steep shock fronts. The code has been applied to a variety of static and dynamic problems, including fracture [84-86]. It is being extended to include sliding surfaces for treatment of penetration problems.

TRIOIL and TRIDORF are both Eulerian three-dimensional finite difference codes, developed by W. E. Johnson [87-88]. They have been applied to the study of shaped charge penetration of finite thickness plates (with the jet modeled as a rigid rod) at high obliquity as well as other problems. Both codes are similar to their predecessors, OIL and DORF, except that TRIDORF is a two-material code with a rigid plastic strength formulation. Similar in spirit is METRIC, developed by Hageman et al [89-90]. The numerical methods and material descriptions are similar to those employed in HELP, its forerunner. The code is not core-contained so that in theory it can provide any degree of spatial resolution. In its initial development, METRIC relied on mixed cells (cells containing more than one material) to establish material boundaries. The code was eventually modified and now material interfaces and free surfaces are defined by massless tracer particles, just as in the HELP code.

Finite element methods based on Eulerian material descriptions are under development by Reddy [91-92] and Chan et al [93]. The latter have developed models that include visco-plastic and strain rate effects and account for material failure. Impact is viewed as a problem in the structural response class and the ultimate goal is the coupling of the Eulerian impact model with a Lagrangian structural response code such as NASTRAN.

The EPIC-3 code developed by G. R. Johnson [94-97] of Honeywell is based on a Lagrangian finite element lumped mass formulation employing tetrahedron elements. As with its two-dimensional analog, EPIC-2, the equations of motion are integrated directly, bypassing the traditional stiffness matrix approach. A fairly comprehensive material description capability exists, allowing for strain hardening, strain rate effects, thermal softening, and fracture. Geometry generators are included to quickly generate flat plates and rods with various nose shapes. Unlike conventional finite element schemes, the first version of EPIC-3 did not require an orderly grid.

In later versions [98], the EPIC-3 code has been restructured into three separate programs: a pre-processor, main processor, and post-processor. All are connected by a common restart tape. Provided that the nodal bandwidth can be core-contained, problems of unlimited size can in theory be run. In practice, there is an upper limit to the problem size tractable since as disc storage becomes large, there is a tendency for the machine to spend most of its running time in data transfers and very little in computation. Cost is also a non-negligible constraint. For smaller problems, where all nodes can be core-contained, an option is provided to bypass this buffering. EPIC-3 has been programmed to eventually run on fourth-generation vector computers and should run somewhat faster than the first version on computers which have some vectorization features.

The newer version has expanded sliding surface capability which includes frictional effects, an improved pre-processing capability which cuts down on user input for slide line and geometry definition and the added capability to automatically generate solid and hollow rods with various nose shapes as well as solid and hollow spheres. Pressure as well as velocity initial conditions may be specified in the updated version. Further developments [99] have resulted in an improved post-processing package, provision for elasto-plastic analysis of orthotropic materials, and incorporation of a material model for treatment of impact into concrete and other geological materials. Anisotropic features are also available in TOODY [100] and in the HELP code [101].

Current developments in this area are noteworthy. Two- and three-dimensional codes using implicit (NIKE2D, NIKE3D) and explicit (DYNA2D, DYNA3D) integration schemes have been developed by J. O. Hallquist [102-107] for solution of problems involving large strains and deformations. Spatial discretization can be accomplished

in a variety of ways. DYNA2D, for example, permits a choice of constant stress finite elements that can be degenerated into triangular zones, constant pressure variable node elements, nine-node Lagrangian elements or finite difference zones based on the HEMP difference equations. A general slide line capability is implemented that admits frictional sliding along arbitrary, intersecting grid lines. Loading functions admit pressure and shear loadings along a boundary, body force loadings due to spinning and base accelerations and nodal velocity-time histories. An impressive solution to a difficult problem (deformation of an aluminum rod with length-to-diameter ratio of 48 striking a steel plate at 200 m/s and 10° obliquity) is shown in [104].

The above list is by no means complete. It serves mainly to indicate the types of codes available and the range of problems which can be addressed. The previously cited references should be consulted for a more comprehensive listing and description.

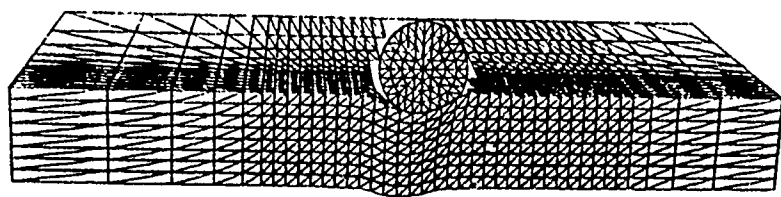
It is not possible to review here the spectrum of calculations which have been done with existing codes. Rather, in the next section, examples of three-dimensional calculations performed at the US Army Ballistic Research Laboratory are presented.

#### IV. EXAMPLES

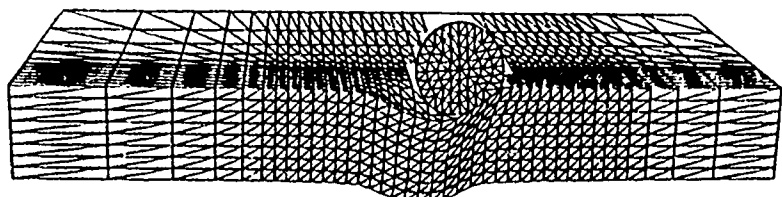
##### A. Sphere Ricochet

In certain impact situations it becomes necessary to account for the effects of friction on the motion of colliding bodies. Figure 6 shows isometric plots of EPIC-3 results for the case of an SAE 52100 steel sphere, 0.635cm in diameter, striking a 2024-T3510 aluminum plate, 0.635cm thick at an obliquity of 60° from the plate normal at a velocity of 720 m/s. Experimental data for this problem is given by Backman and Finnegan [108]. The problem was first addressed computationally by G. R. Johnson [96] with the early version of EPIC-3 using a frictionless sliding interface. Despite a very coarse grid, good agreement was obtained for the deformed profile of target plate. The present calculation was done with a finer grid (5202 nodes and 24576 elements) with the current version of EPIC-3. A computation was also made with a grid consisting of 14768 nodes and 75168 elements, but results did not differ appreciably from the identical case with the 24576 element configuration.

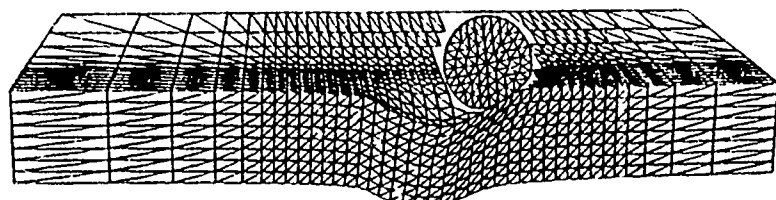
The variation of projectile velocity with time and sliding friction coefficient is shown in Figure 7. For the frictionless interface, the computed residual velocity differs by some 38% from the value of 303 m/s reported by Backman and Finnegan. Progressive increase in the surface friction coefficient reduces the residual velocity of the sphere (and imparts a correspondingly greater spin to it). At 25% friction, the computed residual velocity of 318 m/s differs by less than 5% from that reported experimentally. The deformation pattern in the target is little affected by the frictional interface and is substantially the same for all cases.



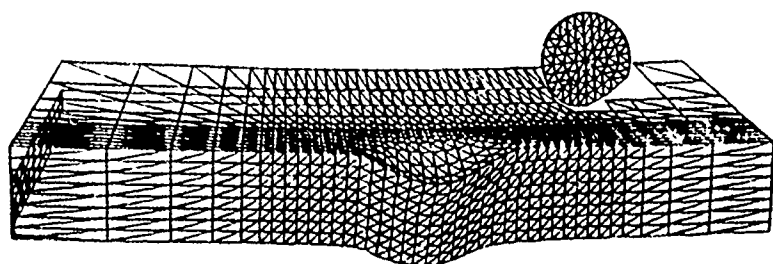
5 Microseconds



10 Microseconds



15 Microseconds



40 Microseconds

Figure 6. Deformation profiles for oblique impact of steel sphere into aluminum target at various times

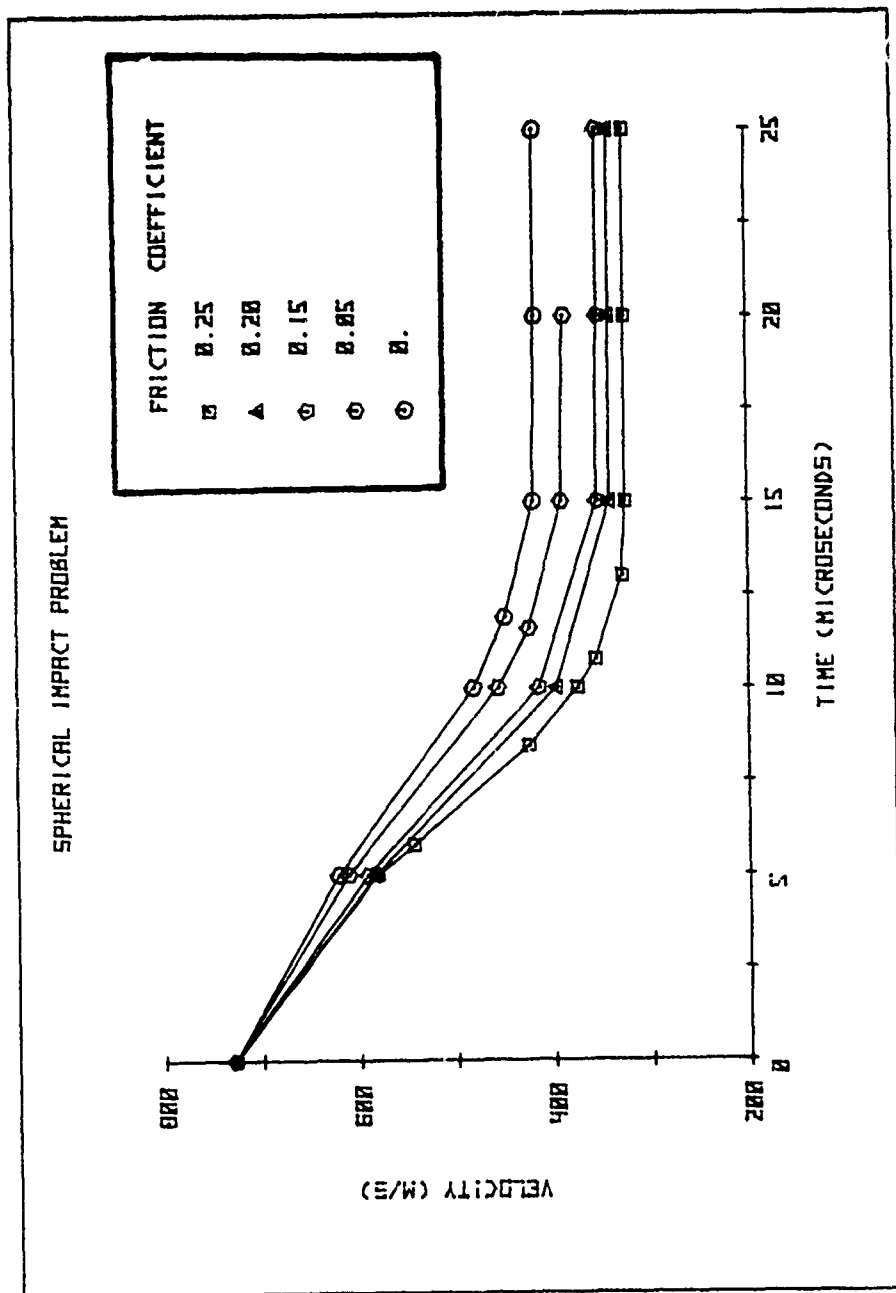


Figure 7. Velocity histories for oblique impact of steel sphere into aluminum target

In actual fact, the surface friction effect would be a function of the relative velocity of the impacting bodies. It is unlikely to be significant at impact velocities  $> 1 \text{ km/s}$  where very high pressures are generated at the impact interface producing a thin layer of material which acts as a fluid. At lower velocities and for drawing and punching problems frictional effects can be significant. Estimates of frictional coefficients are not easily obtained, however. In a recent paper [109] Ghosh determined the coefficient of friction for sheets of various materials being struck by a hemispherical steel punch. Average values of the coefficient of friction were calculated for a number of materials under various conditions of lubrication. The aluminum alloys considered were 2036-T4, 3003-0, and 5182-0 aluminum. The calculated coefficient of friction for these alloys ranged from 0.22-0.41 for the dry state and from 0.07-0.27 for test pieces coated with Teflon and polyethylene. With these results in mind and the close agreement with experiment for projectile residual velocity and target deformed shape, it is proper to conclude that EPIC-3 results are a quite reasonable approximation of the principal features of the impact event.

All the computations were done on a CDC 7600 computer. Typical running times for all but the fine grid problems were just under two hours.

#### B. Yawed Rod Impact

It is now well established that impact encounters at large yaw angles seriously degrade the performance of long rod strikers [110]. Knowledge of the deformations and stress states which occur under such conditions can prove valuable in understanding rod behavior and improving projectile design.

The specific problem considered here involves the impact of a 2024-T3510 aluminum rod (length 5.57cm, diameter 0.635cm) by a circular plate (diameter 10.16cm, thickness 1.27cm) of rolled homogeneous armor at a velocity of 550 m/s. The rod was suspended by tungsten wires in a plastic frame at an angle of 45°. A four inch gas gun was used to launch the plate against the stationary rod. A xenon flash source was used for back lighting and the event photographed at two microsecond intervals with a Cordin model 330 framing camera.

Figure 8 shows a comparison of experimentally recorded deformation profiles with those computed by EPIC-3 at two different times. A total of 1992 nodes and 8304 tetrahedral elements were used for the calculation. The agreement is generally excellent. For the later time, it is seen that the curvature of the deformed portion of the rod does not quite match that shown in the framing camera

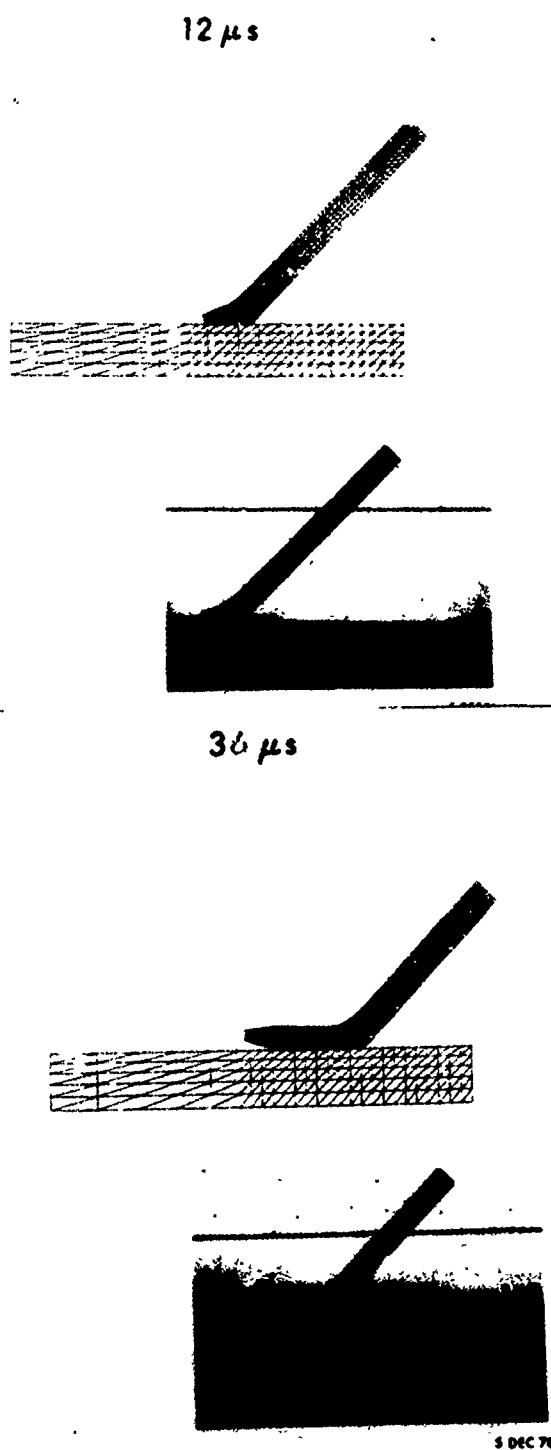


Figure 8. Rod deformation at various times

record. This is due to inadequate numerical resolution in that portion of the rod, which experiences severe stress gradients. The same problem was rerun doubling the number of elements in the projectile. For this case, the computed and experimental deformation profiles matched exactly to 24  $\mu$ s, at which point the calculation was terminated. As before, the calculation was performed on a CDC 7600 and required a little over two hours to compute rod response to 60  $\mu$ s. Material properties for the computations were obtained from the free-flight impact experiments of Bell [111].

### C. Hydrodynamic Ram

Hydrodynamic ram refers to the high pressures that are developed when a fluid reservoir is penetrated by a kinetic energy (KE) projectile. Hydrodynamic ram in aircraft fuel cells can damage structural components or rupture tank walls which in turn can lead to fuel starvation, fire, and explosion.

The hydrodynamic ram event is generally considered to consist of a shock phase, a drag phase, a cavitation phase, and an exit phase. The shock phase occurs during initial impact with the fluid at which time the projectile impulsively accelerates the fluid and generates an intense pressure field bounded by a hemispherical shock wave. This shock wave expands radially away from the impact point and may produce petalling of the entrance panel. As the projectile traverses the fluid it transfers a portion of its momentum to the fluid as it is decelerated due to viscous drag. If the projectile tumbles in the fluid, a significantly larger portion of the projectile's momentum will be transferred to the fluid. The radial velocities imparted to the fluid during the drag phase lead to the formation of a cavity behind the penetrator. This is often termed the cavitation phase. As the fluid seeks to regain its undisturbed condition, the cavity will oscillate. The time interval during which the exit panel of the fluid cell is perforated by the KE projectile is referred to as the exit phase.

Kimsey [112] has employed the EPIC-2 code to study the impact of an S7 steel rod into a cylindrical fuel cell simulator. The rod was a right circular cylinder with a hemispherical nose, weighed 50 grams, had a length-to-diameter ratio of 3 and was assumed to strike the fluid-filled container normally at a velocity of 909 m/s. The outer diameter of the container was taken to be 50.8cm, its depth was 15.2cm and the wall thickness (2024-T3 aluminum) was 1.8mm. The fluid was simulated as water. Sliding was permitted between the projectile and the water as well as between the water and the interior portions of the entrance and exit panels of the simulator. 2943 nodes and 5424 triangular elements were used for the simulation.

Deformation and pressure profiles at 40 and 180  $\mu$ s after impact [112] are shown in Figure 9. The impulsive acceleration of the fluid during the shock phase (10  $\mu$ s after impact) generates peak pressures of 280 MPa, which decay rapidly to 14 MPa and persist at about that level during the drag phase. Pounding of the entrance panel due to the action of the water is also evident. By 180  $\mu$ s, the exit panel has been sufficiently loaded to initiate bulging prior to perforation. The entrance panel has been deflected considerably and an additional cavity between the entrance panel and the water has formed. The cavity formed behind the water was formed by permitting total failure of elements which exceed an equivalent strain of 2.5.

No experimental data for this case was found. However, Kimsey was able to compare the predicted residual velocity from EPIC-2 with that determined from an empirical relationship derived on the basis of a number of hydrodynamic ram experiments. The two values differed by 4%.

#### V. COMPUTATIONAL FAILURE MODELS

The most serious limitation to extensive use of computational techniques described above arises not from their cost or complexity (ballistic experiments are neither less costly nor less complex) but from the inadequacy of the models describing material failure. Under dynamic loading, failure can occur by a variety of mechanisms dependent on the material constitution and the state of stress, temperature, rate of loading, and a number of other variables. The methods and results of quasi-static fracture studies are of little use in situations involving high rate loading.

Simple empirical failure models of varying degrees of complexity exist. Some have been applied successfully in high velocity impact calculations. For the most part, though, failure criteria and models are of an ad hoc nature, lacking a micromechanical basis to treat comprehensively problems involving brittle, ductile, and shear failure. Different criteria apply for different impact conditions and there are at present no guidelines to analysts for selecting an appropriate failure criterion under different conditions.

Computational failure models for impact loading situations are discussed in recent review articles [113, 3] and in some depth in a report by the National Materials Advisory Board Committee on Materials Response to UltraHigh Loading Rates [114]. Hence, the following remarks are intended to summarize the current state of affairs in numerically simulating material failure. The cited references should be consulted for additional details.

It is now generally accepted that material failure under impact loading is a time-dependent phenomenon. Experimental observations lead to the following conclusions about the general features of materials failure [113]:

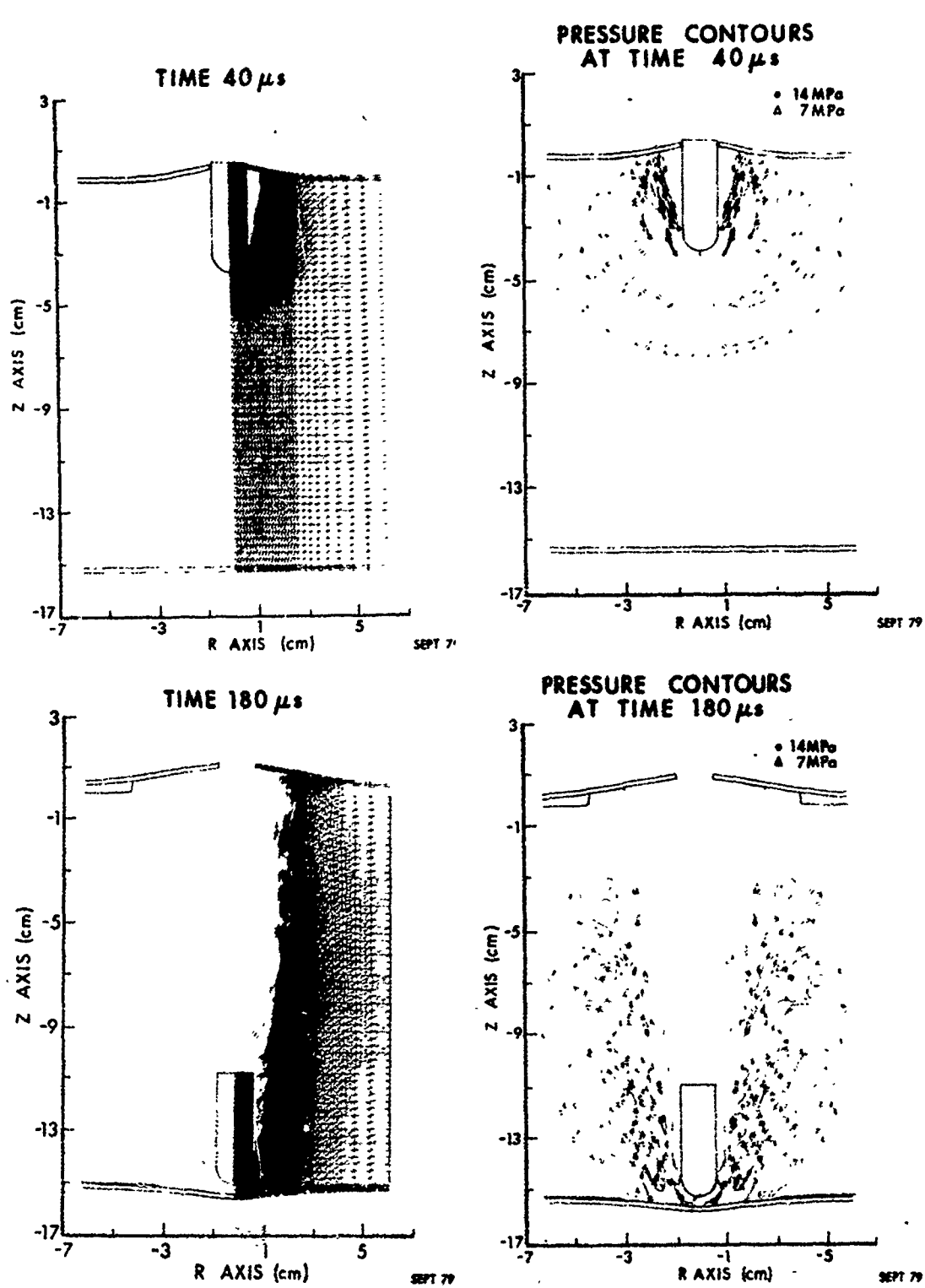


Figure 9. Deformations and pressures in fuel tank simulator at 40 to 180  $\mu$ s

a. a range of damage is possible; there is no instantaneous jump from undamaged to fully separated material.

b. damage grows as a function of time and the applied stress. Hence, a single field variable of continuum mechanics (stress, strain, plastic work, etc.) at any time cannot be expected to characterize the dynamic fracture process. At least some time-integral quantity must be used to represent the dynamic strength. Of course, if the intensity of the applied load is so severe that the damage occurs in negligibly short time, reasonable results may be expected from instantaneous failure criteria.

c. as the level of damage increases, the material is weakened and its stiffness reduced. This changes the character of the wave propagation through the material. Ideally, this should be accounted for in computational procedures.

d. even incipient damage levels are important since voids or cracks, difficult though they may be to observe, may seriously weaken a structure.

There are a number of failure descriptions used in current production codes. They involve an initiation criterion and some description of the post-failure behavior.

The simplest of the initiation criteria are based on instantaneous values of a field variable, such as pressure, stress, strain, plastic work, or some combination thereof. Once the criterion has been satisfied at a given location, failure is considered to occur instantaneously. The post-failure response can be described in a number of ways. The failed material may be entirely removed from the computation or be described by a modified constitutive function which describes a weakened material.

One of the simplest of such models, for example, is the pressure cutoff. When the hydrostatic pressure reaches a critical tensile value (or zero), failure is assumed to occur instantaneously. Further expansion occurs at that fixed value of pressure. If subsequently recompression occurs, compressive pressures are again allowed. More complicated versions of this basic approach have been implemented. Excellent results have been obtained with critical stress criteria [24] for hypervelocity impact situations where dynamic tensile spall situations exist.

Time-dependent initiation criteria represent the next level of sophistication and have been successfully applied in several situations. One of the earliest is due to Tuler and Butcher [115]. Failure is assumed to occur instantaneously when a critical value of the damage  $K$ , defined by the integral

$$K = \int_0^t (\sigma - \sigma_0)^\lambda dt \quad (5)$$

is reached. Here  $\sigma(t)$  is a tensile stress pulse of arbitrary shape,  $\sigma_0$  a threshold stress level below which no significant damage will occur regardless of stress duration and  $\lambda$  is considered a material-dependent parameter chosen to fit experimental data. The parameters  $\lambda, \sigma_0$  and  $K_{\text{critical}}$  are taken to be material parameters which must be determined from separate experiments.

Criteria in which the damage accumulation is a function of the extent of damage as well as field variables have also been devised [116]. Here the damage accumulation function is taken to be a function of strain, temperature, and the current damage level

$$\dot{K} = f(\epsilon, T, K) \quad (6)$$

and the post-failure description includes progressive weakening of the material as the damage increases.

In an attempt to include micromechanical behavior in a continuum damage model, researchers at SRI International [114, 117-119] have developed models for ductile, brittle and shear failure. For ductile failure damage is initiated when the average stress exceeds a tensile pressure criterion. Brittle fracture is initiated when the maximum normal stress exceeds a tensile threshold. Shear banding begins when the maximum plastic shear strain exceeds a critical value. After initiation, voids, cracks or shear bands nucleate and grow according to experimentally determined rate equations. These equations are determined from experiments in which samples are exposed to pulse loads of varying amplitudes and durations. The samples are then sectioned and examined metallographically to measure the microcrack, void or shear band size and orientation distributions as a function of the imposed stress and strain histories. Calculations are made by storing the crack, void or shear band size and orientation distributions for each location. These distributions serve as internal state variables. As the damage accumulates, the stresses are relaxed by amounts and in directions governed by the damage distribution functions. The brittle fracture and shear banding models have been extended to predict fragment size distributions on complete failure, based on very simple descriptions of the coalescence of individual flaws.

It is clearly established that the material descriptions which most affect computational results are the flow stress and the failure model. This latter aspect is especially evident in the computations performed by Gupta and Misey [20]. They used the EPIC-2 finite element Lagrangian code and the HELP finite difference Eulerian code to study surface strains in long rods during penetration. Computational results with EPIC-2 in which failure was not allowed to occur showed little resemblance to experimentally determined strain-time records. When a failure criterion based on effective plastic strain was included, good agreement was obtained between computed and experimentally

determined strain-time records. Computations with the HELP code used a failure criterion based on a minimum allowable density ratio. In general, better agreement with experimental results was obtained with the finite element code using an effective plastic strain failure criterion than with the finite difference code with failure based on a density ratio.

For lack of any substantive theoretical guidance, most computations are performed with the simplest available failure criteria. These generally require the least amount of material characterization and are easily implemented in computer codes. Too often, the failure criterion is used as an adjustable parameter to bring into coincidence computational and experimental results, with the ensuing argument that the close agreement is proof of the applicability of the particular model and data chosen. Such arguments can and should be dismissed out of hand. This is most easily done for situations where the failure model has no micromechanical basis. But in general the tendency to treat material descriptors as adjustable parameters should be discouraged. A quote from a recent paper [120] very succinctly points up the fallacy of this approach: "...the proliferation of parameters, with the aim of providing plausible physical explanation for discrepancies between theory and experiment, has its limitations. In this connection, we were recently reminded of a comment attributed to the French mathematician, Cauchy, to the effect that, given four parameters, he could draw a credible version of an elephant and given five, he could make its tail wiggle."

Problems of accounting for dynamic material behavior and fracture are difficult but not insurmountable, even in view of our present limited knowledge. A practical approach is suggested in the NMAB report [114]. It is suggested that the iterative procedure of successive refinements involving computations with existing relatively simple failure descriptions, dynamic materials characterization employing relatively simple and standardized techniques such as those described in the previous section, and ballistic test firings may produce useful results for design purposes in many applications. The report suggests that "...rough computations, using simple material models with published or even estimated material properties, may be used in conjunction with exploratory test firings to scope an initial design. Comparison of test data with the predictions may reveal discrepancies which suggest refinements in the computations or material models, and the need for some dynamic material property measurements. Once reasonable agreement has been achieved, another round of computations may then be performed to refine the design. Test firings of this design might use more detailed diagnostic instrumentation. This sequence is iterated, including successively more detail in computational models, material property tests and ordnance test firings, until a satisfactory design is achieved. In this procedure, unnecessarily detailed computations, material

property studies or test firings are minimized; only the details necessary to achieve a satisfactory design are included."

The ultimate solution to the problem requires development of micromechanical failure theories through theoretical and experimental research. It is not likely that this will occur even within the next decade. In the interim, the iterative method described above appears to be a practical approach for rational and cost-effective design of materials and systems which must withstand high-intensity impact loading.

## VI. PROGNOSIS

A summary of the state of affairs is in order before hazarding a few opinions on developments which may be anticipated in the near future:

a. the study of impact processes encompasses a wide range of materials responses which cross traditional academic boundaries. Because of the complexity of the subject, no comprehensive solution to impact problems in all velocity regimes exists. Analytical models have very restricted application because of the simplifying assumptions employed in their derivation. The bulk of the work in this area is experimental in nature.

b. many of the ballistic tests which are performed have specific objectives in mind. Data is gathered to satisfy those objectives. Because of this limited scope, such experiments add little to our knowledge of impact processes. The information collected from routine ballistic tests concerns the initial and final states of striker and target (too often, the latter information is obtained from post-mortem examinations). Time and cost constraints do not generally permit acquisition of a data base to permit either development of unambiguous approximate analytical models or confirmation or rejection of the various material descriptions used in present computer codes. Techniques such as instrumented impact tests and cineradiography provide time-resolved information on stress, strain, and deformation states in colliding materials which is of great value in assessing mechanisms governing the impact process and developing models. At present, though, these methods are still in their infancy and quite expensive.

c. numerical techniques offer the hope of obtaining a complete solution to impact problems. Computational techniques have advanced to the point where extremely difficult situations can be analyzed quickly and cost-effectively. Typically, one-dimensional problems can be run in minutes on computers such as the CDC 7600, two-dimensional problems in tens of minutes to a few hours, and three-dimensional problems in a few hours to tens of hours.

d. within broad limits, the geometry of a given problem poses no barrier to computations. In situations where material failure is not a major problem, computations with simple material models for elastic-plastic behavior produce excellent qualitative and quantitative results, especially when care is taken to characterize the materials involved under dynamic conditions appropriate to the problem. A number of standard methods are available for such characterization and a small but growing data base for the behavior of technologically significant alloys at high strain rates already exists.

e. hypervelocity impact situations readily lend themselves to computations. Here, the principal factor in characterizing material behavior is the equation of state. Excellent work in this area has been done over the past three decades and accurate equation of state data now exists for a wide variety of materials and loading conditions. Good material characterization here leads to good qualitative and quantitative results.

f. the description of dynamic material behavior, especially material failure under high loading rates, remains the greatest single limitation on the accuracy and utility of computer codes for solid-solid impact situations.

g. despite lingering uncertainties about the short-duration loading response and failure characteristics of materials, practical solutions of an ad hoc nature for difficult problems involving material failure can be obtained by the iterative use of computations, dynamic material characterization and ballistic testing.

In short then, a clever analyst with access to a large computer, dynamic materials data, and a ballistic test facility can obtain an engineering solution to almost any problem involving the intense impulsive loading of a material or structure, even though the solution may be of an ad hoc nature. What refinements does the future hold for this state of affairs?

The probable situation with regard to computing is somewhat easier to predict. The trend in computer hardware has been towards increased capability at ever-decreasing cost. Three-dimensional impact simulations involving penetration or perforation of solids can now be run in 4-10 hours of CPU time on a CDC 7600 computer. The CRAY-1 computer, now operational at a number of sites, is estimated to be 7-10 times faster than the CDC 7600 for comparable problems. Further developments of large mainframes should result in even greater increases in speed and memory capacity. Thus, hardware developments alone should bring computing times for three-dimensional penetration problems to under one hour of CPU time within the next five years.

In addition, there is considerable activity in developing numerical schemes which are both fast and accurate for problems involving large stress and velocity gradients. Hallquist's work at Lawrence Livermore Laboratory has already been mentioned. Hicks at Sandia Laboratories has developed a two-dimensional wave propagation code using shock fitting techniques [121]. He has also made promising progress in three-dimensional impact calculations. In many impact situations, there is very little activity in a large part of the mesh. Typically, only 5% of the mesh has significant stress or velocity gradients which must be adequately resolved. In explicit schemes, these regions determine the size of time step. This is then used for the entire grid. Using operator splitting and implicit techniques, Hicks was able to use a big time step in a large portion of the grid. In regions of intense activity, subcycling was employed to pick up the necessary time resolution. These methods are still experimental in nature. However, the running time for a three-dimensional impact problem using the above approach was approximately 1/20 that of an explicit scheme [122]. Other methods are under development which would use both implicit and explicit methods. Explicit integration would be used in the early stages of impact where stress or velocity gradients need to be resolved. As the activity then decayed and high frequency components were no longer significant, implicit schemes with their larger time step would then be used to obtain the overall dynamic response of the structure. The combination of improved hardware and innovative software development should make three-dimensional computations routine within the next decade since their cost will become an insignificant portion of the overall project costs.

Development of software for pre- and post-processing of computational results will also be accelerated as CPU costs decline. Development of interactive graphics software for automatic mesh generation and graphical analysis of computational results is an expensive proposition but constitutes a one-time cost, well justified by savings of an analyst's time. Software which places an unnecessary burden on an analyst's time is being gradually replaced. Situations which were common only a few years ago where a week or more was required to prepare input, and several weeks to analyze the output of a two-hour computer run can no longer be logically or economically justified.

The minicomputer will play a significant role in three-dimensional impact computations. Minicomputers with their associated mass storage and graphics capability can be used as hosts for elaborate pre- and post-processing packages for production codes. Once meshes have been generated interactively, computations may be done in batch on a mainframe and the results returned to the minicomputer for post-processing. Alternatively, the minicomputer itself may be used for the computations. Although slower than current mainframes, a minicomputer dedicated to a particular code

can readily be justified on the basis of cost and manpower savings. Both the HEMP and TOODY codes will shortly be operational on mini-computers.

The ability to routinely perform three-dimensional impact calculations at moderate cost will fuel a demand for high strain rate materials data and better descriptions of materials failure at high loading rates. This should soon result in a substantial data bank of dynamic properties (at strain rates up to  $10^4 \text{ s}^{-1}$ ) for many materials, similar to the situation which now exists with equation of state data. Development of failure models with a firm micromechanical basis will remain a formidable task. Impressive work is being done at a number of research centers along this line and it is not unreasonable to expect that first-order models suitable for engineering applications for metals under impact loading may be available within a decade, even though they are likely to be semi-empirical in nature.

Ballistic testing will remain a labor-intensive undertaking. Little reduction in cost can be expected here, but with the availability of advanced instrumentation techniques and the use of minicomputers for automated data acquisition, reduction, and reporting, both the quality and quantity of test data should be improved considerably. This in turn will spur development of approximate analytical techniques and refinement of material descriptions in computer codes.

No one method-computations, ballistic testing, dynamic materials characterization-will by itself lead to fuller understanding of the mechanisms which govern the behavior of materials and structures subjected to intense impulsive loading. The judicious combination of all three can, however, lead to significant advances of our understanding of short-time response phenomena and result in designs capable of withstanding such severe environments. This requires a commitment in money and time-and a fair amount of coordination-by upper level management in both government and industry. It remains to be seen whether the challenge will be met.

#### ACKNOWLEDGMENT

The author wishes to express his gratitude to Messrs. K. D. Kimsey, G. H. Jonas, and G. Silsby for reviewing and criticizing portions of the report. Special thanks are due to Mrs. Helen Bolen for her diligent and meticulous preparation of the report.

## REFERENCES

1. Goldsmith, W., Impact, Edward Arnold, London, 1960.
2. Backman, M.E. and Goldsmith, W., "The Mechanics of Penetration of Projectiles into Targets," Int. J. Engng. Sci., V16, pp 1-99, 1978.
3. Jonas, G.H. and Zukas, J.A., "Mechanics of Penetration: Analysis and Experiment," Int. J. Engng. Sci., V16, pp 879-903, 1978.
4. Backman, M.E., Terminal Ballistics, NWC TP 578, February 1976.
5. Shockley, D.A., Curran, D.R., DeCarli, P.S., "Damage in Steel Plates From Hypervelocity Impact. I. Physical Changes and Effects of Projectile Material," J. Appl. Phys., V46, #9, pp 3766-3775, September 1975.
6. Grabarek, C. and Herr, L., "X-Ray Multi-Flash System for Measurement of Projectile Performance at the Target," BRL TN 1634, September 1966 (AD 807619).
7. Herr, L. and Grabarek, C., "Standardizing the Evaluation of Candidate Materials for High L/D Penetrators," ARBRL-MR-02860, September 1978 (AD A062101).
8. Lambert, J.P. and Ringers, B.E., "Standardization of Terminal Ballistics Testing, Data Storage and Retrieval," ARBRL-TR-02066, May 1978. (AD A056366)
9. Wenzel, A.B. and Dean, J.K., "Behind Armor Spallation Tests," BRL-CR-262, September 1975. (AD B008120L)
10. Arbuckle, A.L., Herr, E.L., and Ricchiazzi, A.J., "A Computerized Method of Obtaining Behind-the-Target Data from Orthogonal Flash Radiographs," BRL-MR-2264, January 1973 (AD 908362L).
11. Ringers, B.E., "Establishment of a Kinetic Energy Penetrator Data Base and Automated Retrieval of Range Data," to appear as a BRL Technical Report.
12. Lambert, J.P., "The Terminal Ballistics of Certain 65 Gram Long Rod Penetrators Impacting Steel Armor Plate," ARBRL-TR-02072 May 1978. (AD A057757)
13. Bracher, R.J. and Huston, A.E., "High Speed Radiography of Projectiles," Proc. 12th Cong. on High Speed Photography, 1-7 August 1976, pp 532-537.
14. Hadland, R., "Techniques and Applications of Image Converter Cameras," Proc. 13th Int. Cong. on High Speed Photography and Photonics, 20-25 August 1978, Tokyo, Japan, pp 151-161.
15. Bracher, R.J. and Swift, H.F., "X-Ray Cinematography-An Engineering Diagnostic Tool," Proc. ICIASF Conf., 1979.
16. Swift, H.F., "Survey of Recent High-Speed Photographic Developments in North America," Proc. 13th Int. Cong. on High Speed Photography and Photonics, 20-25 August 1978, Tokyo, Japan, pp 8-19.
17. Hauver, G.E., "Penetration with Instrumented Rods," Int. J. Engng. Sci., V16, pp 871-877, 1978.

18. Hauver, G.E. and Melani, A., "Strain-Gauge Techniques for Studies of Rod Behavior During Penetration," to appear as a BRL Technical Report.
19. Netherwood, P., "Rate of Penetration Measurements," to appear as a BRL Memorandum Report.
20. Gupta, A.D. and Misey, J.J., "Comparative Evaluation of Structural Response at High Strain Rates Using Eulerian and Lagrangian Hydrodynamic Codes," AIAA Paper 80-0403, presented at AIAA 18th Aerospace Sciences Meeting, 14-16 January 1980, Pasadena, CA.
21. Venable, D. and Boyd, Jr., T.J., "PHERMEX Applications to Studies of Detonation Waves and Shock Waves", Proc. 4th Int. Symp. on Detonation, 12-15 October 1965, Naval Ordnance Laboratory, White Oak, MD, ACR-126, US Government Printing Office, 1965.
22. Recht, R.F., "Quasi-Empirical Models of the Penetration Process," Joint Technical Coordinating Group for Munitions Effectiveness, JTCG/ME Working Party for KE Penetrators, Information Exchange Meeting, 13-14 February 1973 at USA Ballistic Research Laboratories, Aberdeen Proving Ground, MD.
23. Baker, W.E., Westine, P.S. and Dodge, F.T., Similarity Methods in Engineering Dynamics, Spartan Books, Rochelle Park, NJ, 1973.
24. Bertholf, L.D. et al, "Damage in Steel Plates from Hypervelocity Impact. II. Numerical Results and Spall Measurement," J. Appl. Phys., V46, #9, pp 3776-3783, September 1975.
25. Roddy, D.J., Peppin, R.O., and Merrill, R.B. eds., Impact and Explosion Cratering, Proceedings of a Symposium on Planetary Cratering Mechanics, Flagstaff, AZ, 13-17 September 1976, Pergamon Press, NY, 1977.
26. Mescall, J.F., "Shock Wave Propagation in Solids," Structural Mechanics Computer Programs, ed. W. Pilkey, S. Saczalski and H. Schaeffer, U. of Virginia Press, Charlottesville, VA, 1974.
27. Zienkiewicz, O.C., The Finite Element Method in Engineering Science, McGraw-Hill, London, 1971.
28. Chang, J.W., "Structural Dynamics in LMFBR Containment Analysis. A Brief Survey of Computational Methods and Codes," Proc. 4th Int. Conf. on Structural Mechanics in Reactor Technology, Vol E, Part 1, T.A. Jaeger and B.A. Boley, eds., North-Holland, 1977.
29. Belytschko, T., "Computer Methods in Shock and Wave Propagation Analysis," Computing in Applied Mechanics, R. F. Hartung, ed., pp 139-161, AMD, V18, ASME, NY, 1977.
30. Herrmann, W. and Hicks, D.L., "Numerical Analysis Methods," Metallurgical Effects at High Strain Rates, ed. R.W. Rhode, B.M. Butcher, J.R. Holland, and C.H. Karnes, Plenum Press, NY, 1973.
31. Herrmann, W., Bertholf, L.D., and Thompson, S.L., "Computational Methods for Stress Wave Propagation in Nonlinear Solid Mechanics," ed. J.T. Oden, Springer-Verlag, NY, 1975.
32. Herrmann, W., "Nonlinear Transient Response of Solids," Shock and Vibration Computer Programs, Reviews and Summaries, ed. W. and B. Pilkey, Shock and Vibration Information Center, Naval Research Laboratory, Washington, DC, 1975.

33. Herrmann, W., Hicks, D.L., and Young, E.G., "Attenuation of Elastic-Plastic Stress Waves," Shock Waves and the Mechanical Properties of Solids, ed. J.J. Burke and V. Weiss, Syracuse U. Press, 1971.

34. Walsh, K.T., "Finite-Difference Methods," Dynamic Response of Materials to Intense Impulsive Loading, ed. P.C. Chou and A.K. Hopkins, US Government Printing Office, 1972.

35. Argyris, J.H., Doltsinis, J. St., Knudson, W.C., Vaz, L.E., and William, K.J., "Numerical Solution of Transient Nonlinear Problems," Comp. Methods in Appl. Mech. and Engr., V17/18, pp 341-409, 1979.

36. Herrmann, W., "Current Problems in the Finite Difference Solution of Stress Waves," Proceedings of the Workshop on Nonlinear Waves in Solids, T.C.T. Ting, R.J. Clifton, and T. Belytschko, eds., National Science Foundation, 1977.

37. Courant, R., Friedrichs, K.O., and Lewy, H., "Über die Partialen Differenzen-gleichungen der Matematischen Physik," Math. Ann. 100 1928.

38. Van Thiel, M., "Compendium of Shock Wave Data," Lawrence Livermore Laboratory, UCRL-50108, V I-III, 1977.

39. Kohn, B.J., "Compilation of Hugoniot Equations of State," Air Force Weapons Laboratory, AFWL-TR-69-38, April 1969 (AD 852300).

40. Lee, E.H., "Plastic-Wave Propagation Analysis and Elastic-Plastic Theory at Finite Strain," Shock Waves and the Mechanical Properties of Solids, ed. J.J. Burke and V. Weiss, Syracuse U. Press, 1970.

41. Green, A.E. and Naghdi, P.M., "A General Theory of an Elastic-Plastic Continuum," Arch. Rational Mech. Anal., V18, 1965.

42. Armen, H., "Assumptions, Models, and Computational Methods for Plasticity," Computers and Structures, V10, pp 161-174, 1979.

43. Wilkins, M.L., "Calculation of Elastic-Plastic Flow," Methods in Computational Physics, V3, ed. B. Alder, S. Fernbach, and M. Rotenberg, Academic Press, NY 1964.

44. Johnson, G.R., Colby, D.D., and Vavrick D.J., "Further Development of the EPIC-3 Computer Program for Three-Dimensional Analysis of Intense Impulsive Loading," Air Force Armament Laboratory, AFATL-TR-78-81, July 1978.

45. Herrmann, W. and Lawrence, R.J., "The Effect of Material Constitutive Models on Stress Wave Propagation Calculations," Trans. ASME, J. Engineering Matls. and Technology, V100, pp 84-95, January 1978.

46. Wilkins, M.L. and Guinan, M.W., "Impact of Cylinders on a Rigid Boundary," J. Appl. Phys., V94, #3, pp 1200-1206, March 1973.

47. Norris, D. M., Scudder, J. K., McMaster, W.H., and Wilkins, J.L., "Mechanics of Long Rod Penetration at High Obliquity," Proceedings of the High Density Alloy Penetrator Materials Conference, Army Materials and Mechanics Research Center, AMMRC-SP-77-3, April 1977.

48. Lindholm, U.S., "High Strain Rate Testing," Techniques of Metals Research, V5, Part 1, R.F. Bunshah, ed., Wiley, 1971.

49. Bertholf, L.D. and Karnes, C.H., "Two-Dimensional Analysis of the Split Hopkinson Pressure Bar System," J. Mech. Phys. Solids, V23, pp 1-19, 1975.

50. Bushan, B. and Jahsman, W.E., "Measurement of Dynamic Material Behavior Under Nearly Uniaxial Strain Conditions," Int. J. Solids Structures, V14, pp 739-753, 1978.

51. Nicholas, T., "Mechanical Properties of Structural Grades of Beryllium at High Strain Rates," Air Force Materials Laboratory, AFML-TR-75-168, October 1975.
52. Duffy, J., Campbell, J.D., and Hawley, R.H., "On the Use of a Torsional Split Hopkinson Bar to Study Rate Effects in 1100-0 Aluminum," J. Appl. Mech., V38E, pp 83-91, 1971.
53. Lindholm, U.S., "Some Experiments with the Split Hopkinson Pressure Bar," J. Mech. Phys. Solids, V12, pp 317-335, 1964.
54. Bell, J.F., "The Dynamic Plasticity of Metals at High Strain Rates: An Experimental Generalization," Behavior of Materials Under Dynamic Loading, Huffington, N.J. ed., ASME, NY, 1965.
55. Bell, J.F., "On the Direct Measurement of Very Large Strain at High Strain Rates," Exp. Mech., V7, 1967.
56. Bell, J.F., The Physics of Large Deformation of Crystalline Solids, Springer-Verlag, NY, 1968.
57. VonKarman, T. and Duwez, P.E., "The Propagation of Plastic Deformation in Solids," J. Appl. Phys., V21, 1950.
58. Nolle, H., "Significance of Response Characteristics of Materials to Dynamic Loading," Int. Metallurgical Revs., V19, pp 223-239, December 1974.
59. Taylor, G.I., "The Use of Flat-Ended Projectiles for Determining Dynamic Yield Stress. I: Theoretical Considerations," Proc. Roy. Soc. A, V194, pp 289-299, 1948.
60. Whiffen, A.C., "The Use of Flat-Ended Projectiles for Determining Dynamic Yield Stress. II: Tests on Various Metallic Materials," Proc. Roy. Soc. A, V194, p 300, 1948.
61. Hawkyard, J.B., "Mushrooming of Flat-Ended Projectiles Impinging on a Flat, Rigid Anvil," Int. J. Mech. Sci., V11, p 313, 1969.
62. Karnes, C.H., "The Plate Impact Configuration for Determining Mechanical Properties of Materials at High Strain Rates," Mechanical Behavior of Materials Under Dynamic Loads, ed. U.S. Lindholm, Springer-Verlag, NY, 1968.
63. Davison, L. and Graham, R.A., "Shock Compression of Solids," Phys. Reports, V55, #4, pp 257-379, October 1979.
64. vonRiesemann, W.A., Stricklin, J.A., and Haisler, W.E., "Nonlinear Continua," Structural Mechanics Computer Programs, ed. W. Pilkey, K. Saczalski, and H. Schaeffer, U. of Virginia Press, Charlottesville, VA, 1974.
65. Wilkins, M.L., "Calculation of Elastic-Plastic Flow," Lawrence Livermore Laboratory, UCRL-7322, Rev. 1, 1969.
66. Giroux, E.D., "HEMP User's Manual," Lawrence Livermore Laboratory, UCRL-51079, Rev. 1, 1973.
67. Bertholf, L.D. and Benzley, S.E., "TOODY II - A Computer Program for Two-Dimensional Wave Propagation," Sandia Laboratories, SC-RR-68-41, 1969.
68. Thorne, B.J. and Holdridge, D.B., "The TOOREZ Lagrangian Rezoning Code," Sandia Laboratories, SLA-73-1057, 1974.
69. Swegle, J.W., "TOODY-IV - A Computer Program for Two-Dimensional Wave Propagation," Sandia Laboratories, SAND-78-0552, 1978.
70. Johnson, G.R., "EPIC-2, A Computer Program for Elastic-Plastic Impact Computations in 2 Dimensions Plus Spin," USA Ballistic Research Laboratory, ARBRL-CR-00373, 1978 (AD A058786).

71. Hageman, L.J., Wilkins, D.E., Sedgwick, R.T., and Waddell, J.L., "HELP, A Multi-Material Eulerian Program for Compressible Fluid and Elastic-Plastic Flows in Two Space Dimensions and Time," Systems Science and Software, Inc., 1975.
72. Hageman, L.J. and Sedgwick, R.T., "Modification to the HELP Code for Modeling Plugging Failure," Air Force Armament Laboratory, Contractor Report 3SR-1009, Eglin AFB, FL, 1972.
73. Hageman, L.J. and Herrmann, R.G., "Incorporation of the NAG-FRAG Model for Ductile and Brittle Fracture into HELP, a 2D Multi-Material Eulerian Program," USA Ballistic Research Laboratory, ARBRL-CR-00380, 1978. (AD A062335)
74. Sedgwick, R.T., Hageman, L.J. Herrmann, R.G., and Waddell, J.L., "Numerical Investigations in Penetration Mechanics," Int. J. Engng. Sci., V16, #10-11, pp 859-870, 1978.
75. Schmitt, J.A., "A New Internal Energy Calculation for the HELP Code and its Implications to Conical Shaped Charge Simulation," USA Ballistic Research Laboratory, ARBRL-TR-02168, 1979. (AD A072785)
76. Durrett, R.E. and Matuska, D.A., "The HULL Code. Finite Difference Solution to the Equations of Continuum Mechanics," Air Force Armament Laboratory, AFATL-TR-78-125, 1978.
77. Gaby, L.P., "HULL System Guide," Air Force Weapons Laboratory, C4-C-4041, 1978.
78. Johnson, W.E., "Code Correlation Study," Air Force Weapons Laboratory, AFWL-TR-70-144, 1971.
79. Johnson, W.E., "Development and Application of Computer Programs to Hypervelocity Impact," Systems, Science and Software, Inc., 3SR-749, 1971.
80. Thompson, S.L., "CSQ - A Two-Dimensional Hydrodynamic Program with Energy Flow and Material Strength," Sandia Laboratories, SAND-74-0122, 1975.
81. Thompson, S.L., "Input Instructions for CSQ II - A Ten Material Version of CSQ," Sandia Laboratories, RS5166/135, 1975.
82. Bertholf, L.D., Kipp, M.E., Brown, W.T., and Stevens, A.L., "Kinetic Energy Projectile Impact on Multi-Layered Targets: Two-Dimensional Stress Wave Calculations," USA Ballistic Research Laboratory, ARBRL-CR-00391, 1979. (AD B037370L)
83. Wilkins, M.L., Blum, R.E., Cronshagen, E., and Grantham, P., "A Method for Computer Simulation of Problems in Solid Mechanics and Gas Dynamics in Three Dimensions and Time," Lawrence Livermore Laboratory, UCRL-51574, Rev. 1, 1975.
84. Wilkins, M.L., "Fracture Studies with Two- and Three-Dimensional Computer Simulation Program," Proc. Conf. on Fracture Mechanics and Technology, Hong Kong, 21-25 March 1977, Noordhoff Int., Leyden.
85. Chen, Y.M. and Wilkins, M.L., "Stress Analysis of Crack Problems with a Three-Dimensional, Time-Dependent Computer Program" Int. J. of Fracture, V12, #4, pp 607-617, 1976.

86. Chen, Y.M., "Numerical Solutions of Three-Dimensional Dynamic Crack Problems and Simulation of Dynamic Fracture Phenomena by a 'Non-Standard' Finite Difference Method," Engr. Fracture Mech., V10, pp 699-708, 1978.

87. Johnson, W.E., "TRIOIL - A Three-Dimensional Version of the OIL Code," General Atomic, GAMD-7310, 1967.

88. Johnson, W.E., "Three-Dimensional Computations on Penetrator-Target Interactions," USA Ballistic Research Laboratory, BRL-CR-338, 1977.

89. Hageman, L.J., Waddell, J.L., and Herrmann, R.G., "Application of the Multi-Material Eulerian Three-Dimensional Metric Code to Two Ballistic Impact Situations," Systems, Science and Software, Inc., SSS-R-76-2973, 1976.

90. Hageman, L.J. and Lee, E.P., "Development of Ordnance Velocity, Multimaterial, Three-Dimensional Perforation Code for Finite Plates," USA Ballistic Research Laboratory, BRL-CR-305, 1976. (AD B013125L)

91. Reddy, J.N., "Hydrodynamics of Hypervelocity Impact by Finite Element Method," Meeting Reprint #2417, ASCE National Structural Engineering Convention, 14-18 April 1975, New Orleans, LA.

92. Reddy, J.N., "Finite Element Analysis of the Initial Stages of Hypervelocity Impact," Computer Methods in Appl. Mech. and Engng., V9, pp 47-63, 1976.

93. Chan, S.T.K., Lee, C-H., and Brashears, M.R., "Three-Dimensional Finite Element Analysis for High Velocity Impact," NASA-CR-134933, 1975.

94. Johnson, G.R., "Analysis of Elastic-Plastic Impact Involving Severe Distortions," J. Appl. Mech., V98, #3, 1976.

95. Johnson, G.R., "High Velocity Impact Calculations in Three Dimensions," J. Appl. Mech., V99, #1, pp 95-100, 1977.

96. Johnson, G.R., "A New Computational Technique for Intense Impulsive Loads," Proc. 3d Int. Symp. on Ballistic, Karlsruhe, Germany, 1977.

97. Johnson, G.R., "EPIC-3, A Computer Program for Elastic-Plastic Impact Calculations in 3 Dimensions," USA Ballistic Research Laboratory,

98. Johnson, G.R., Colby, D.D., and Vavrick, D.J., "Further Development of the EPIC-3 Computer Program for Three-Dimensional Analysis of Intense Impulsive Loading," Air Force Armament Laboratory, AFATL-TR-78-81, 1978.

99. Johnson, G.R., Vavrick, D.J., and Colby, D.D., "Further Development of EPIC-3 for Anisotropy, Sliding Surfaces, Plotting, and Material Models," ARBRL-CR-00429, May 1980. (AD B048305L)

100. Swegle, J.W. and Hicks, D.L., "An Anisotropic Constitutive Equation for Use in Finite Difference Wave Propagation Calculations," Sandia Laboratories, SAND-79-0382, 1979.

101. Sedgwick, R.T., Waddell, J.L., Hageman, L.J., Gurtman, G.A., and Baker, M., "Influence of ABM Material Properties on Erosion Resulting from Particle Impact," USA Ballistic Research Laboratory, BRL-CR-322, 1976. (AD B016036L)

102. Hallquist, J.O., "NIKE2D: An Implicit Finite-Deformation Finite Element Code for Analyzing the Static and Dynamic Response of Two-Dimensional Solids," Lawrence Livermore Laboratories, UCRL-52678, 1979.

103. Hallquist, J.O., "DYNA2D - An Explicit Finite Element and Finite Guide)," Lawrence Livermore Laboratory, UCRL-52429, 1978.

104. Hallquist, J.O., "Preliminary User's Manuals for DYNA3D and DYNAP (Nonlinear Dynamic Analysis of Solids in Three Dimensions)," Lawrence Livermore Laboratory, UCID-17268, Rev. 1, 1979.

105. Hallquist, J.O., "A Numerical Treatment of Sliding Interfaces and Impact," Computational Techniques for Interface Problems, ed. K.C.Park and D.K. Gartling, AMD - Vol 30, ASME, NY, 1978.

106. Hallquist, J.O., "A Numerical Procedure for Three-Dimensional Impact Problems," Preprint 2956, ASCE Fall Convention and Exhibit, San Francisco, CA, 17-21 October 1977.

107. Hallquist, J.O., "A Procedure for the Solution of Finite-Deformation Contact-Impact Problems by the Finite Element Method," Lawrence Livermore Laboratory, UCRL-52066, 1976.

108. Backman, M. and Finnegan, S., "Dynamics of Oblique Impact and Ricochet of Nondeforming Spheres Against Thin Plates," Naval Weapons Center,

109. Ghosh, A.K., "A Method for Determining the Coefficient Friction in Punch Stretching of Sheet Metals," Int. J. Mech. Sci., V19, pp 457-470, 1977.

110. Bless, S.J., Barber, J.P., Bertke, R.S., and Switft, H.F., "Penetration Mechanics of Yawed Rods," Int. J. Engng. Sci., V16, #10-11, pp 829-834, 1978.

111. Franz, Robert, Solid Mechanics Branch, BRL, private communication.

112. Kimsey, K.D., "Numerical Simulation of Hydrodynamic Ram," ARBRL-TR-02217, February 1980. (AD A083290)

113. Seaman, L., "Fracture and Fragmentation Under Shock Loading," Shock and Vibration Computer Programs, Reviews and Summaries, ed. W. and B. Pilkey, The Shock and Vibration Information Center, 1975.

114. "Materials Response to Ultra-High Loading Rates," Report of the Committee on Materials Response to Ultra-High Loading Rates, National Materials Advisory Board, Publication NMAB-356, 1979.

115. Tuler, R.F. and Butcher, B.M., "A Criterion for the Time-Dependence of Dynamic Fracture," Int. J. Fracture Mech., V4, pp 431-437, 1968.

116. Davison, L.W., Stevens, A.L., and Kipp, M.E., "Theory of Spall Damage Accumulation in Ductile Metals," J. Mech. Phys Solids, V25, pp 11-28, 1977.

117. Seaman, L. and Shockley, D.A., "Models for Ductile and Brittle Fracture for Two-Dimensional Propagation Calculations," Army Materials and Mechanics Research Center, AMMRC-CTR-75-2, 1975.

118. Seaman, L. Curran, D.R., and Shockley, D.A., "Computational Models for Ductile and Brittle Fracture," J. Appl. Phys., V47, pp 4814-4826, 1976.

119. Erhich, D.C., Seaman, L., Shockley, D.A., and Curran, D.R., "Development and Application of Computational Shear Band Model," ARBRL-CR-00416, March 1980. (AD A084029)

120. Glenn, L.A. and Janach, W., "Failure of Granite Cylinders Under Impact Loading," Int. J. Fracture, V13, pp 301-317, 1977.

121. Hicks, D.L. and Madsen, M.M., "SKTWO: A Two-Dimensional Lagrangian Wavecode With Shock Fitting," Sandia Laboratories, SAND-78-1806, 1979.

122. Hicks, D.L., Sandia Laboratories, private communication.

**DISTRIBUTION LIST**

<u>No. of Copies</u>	<u>Organization</u>	<u>No. of Copies</u>	<u>Organization</u>
12	<p><b>Commander</b>  <b>Defense Technical Info Center</b>  <b>ATTN: DDC-DDA</b>  <b>Cameron Station</b>  <b>Alexandria, VA 22314</b></p>	1	<p><b>Commander</b>  <b>US Army Materiel Development and Readiness Command</b>  <b>ATTN: DRCDMD-ST</b>  <b>5001 Eisenhower Avenue</b>  <b>Alexandria, VA 22333</b></p>
1	<p><b>Director</b>  <b>Defense Advanced Research Projects Agency</b>  <b>ATTN: Tech Info</b>  <b>1400 Wilson Boulevard</b>  <b>Arlington, VA 22209</b></p>	10	<p><b>Commander</b>  <b>US Army Armament Research and Development Command</b>  <b>ATTN: DRDAR-TD, Dr. R. Weigle</b>  <b>DRDAR-LC, Dr. J. Frasier</b>  <b>DRDAR-SC, Dr. D. Gyorog</b>  <b>DRDAR-LCF, G. Demittrack</b>  <b>DRDAR-LCA, G. Randers-Pehrson</b>  <b>DRDAR-SCS-M, R. Kwatnoski</b>  <b>DRDAR-LCU, E. Barrieres</b>  <b>DRDAR-SCM, Dr. Bloore</b>  <b>DRDAR-TSS (2 cys)</b></p>
1	<p><b>Director</b>  <b>Defense Nuclear Agency</b>  <b>Arlington, VA 22209</b></p>		<p><b>Dover, NJ 07801</b></p>
1	<p><b>Deputy Assistant Secretary of the Army (R&amp;D)</b>  <b>Department of the Army</b>  <b>Washington, DC 20310</b></p>	1	<p><b>Director</b>  <b>US Army ARRADCOM</b>  <b>Benet Weapons Laboratory</b>  <b>ATTN: DRDAR-LCB-TL</b>  <b>Watervliet, NY 12189</b></p>
1	<p><b>HQDA (DAMA-ARP)</b>  <b>WASH DC 20310</b></p>	1	<p><b>Commander</b>  <b>US Army Armament Materiel Readiness Command</b>  <b>ATTN: DRSAR-LEP-L, Tech Lib</b>  <b>Rock Island, IL 61299</b></p>
1	<p><b>HQDA (DAMA-MS)</b>  <b>WASH DC 20310</b></p>	1	<p><b>Commander</b>  <b>US Army Aviation Research and Development Command</b>  <b>ATTN: DRSAV-E</b>  <b>12th and Spruce Streets</b>  <b>St. Louis, MO 63166</b></p>
2	<p><b>Commander</b>  <b>US Army Engineer Waterways Experiment Station</b>  <b>ATTN: Dr. P. Hadala</b>  <b>Dr. B. Rohani</b>  <b>PO Box 631</b>  <b>Vicksburg, MS 39180</b></p>		

## DISTRIBUTION LIST

<u>No. of Copies</u>	<u>Organization</u>	<u>No. of Copies</u>	<u>Organization</u>
1	Director US Army Air Mobility Research and Development Laboratory Ames Research Center Moffett Field, CA 94035	6	Director US Army Materials and Mechanics Research Center ATTN: DRXMR-T, Mr. J. Bluhm Mr. J. Mescall Dr. M. Lenoe R. Shea F. Quigley DRXMR-ATL Watertown, MA 02172
1	Commander US Army Communications Research and Development Command ATTN: DRDCO-PPA-SA Fort Monmouth, NJ 07703	2	Commander US Army Research Office ATTN: Dr. E. Saibel Dr. G. Mayer PO Box 12211 Research Triangle Park NC 27709
1	Commander US Army Electronics Research and Development Command Technical Support Activity ATTN: DELSD-L Fort Monmouth, NJ 07703	1	Director US Army TRADOC Systems Analysis Activity ATTN: ATAA-SL (Tech Lib) White Sands Missile Range NM 88002
3	Commander US Army Missile Research and Development Command ATTN: DRSMI-R DRSMI-RBL DRSMI-YDL Redstone Arsenal, AL 35809	1	Office of Naval Research Department of the Navy ATTN: Code ONR 439, N. Perrone 800 North Quincy Street Arlington, VA 22217
2	Commander US Army Tank-Automotive Research and Development Command ATTN: DRDTA-UL V. H. Pagano Warren, MI 48090	3	Commander Naval Air Systems Command ATTN: AIR-604 Washington, DC 20360
1	Commander TARADCOM Tank-Automotive Systems Laboratory ATTN: T. Dean Warren, MI 48090	3	Commander Naval Ordnance Systems Command Washington, DC 20360

**DISTRIBUTION LIST**

<u>No. of Copies</u>	<u>Organization</u>	<u>No. of Copies</u>	<u>Organization</u>
2	Commander Naval Air Development Center, Johnsville Warminster, PA 18974	3	Director Naval Research Laboratory ATTN: Dr. C. Sanday Dr. H. Pusey Washington, DC 20375
1	Commander Naval Missile Center Point Mugu, CA 93041	2	Superintendent Naval Postgraduate School ATTN: Dir of Lib Dr. R. Ball Monterey, CA 93940
2	Naval Ship Engineering Center ATTN: J. Schell Tech Lib Washington, DC 20362	1	Long Beach Naval Shipyard ATTN: R. Kessler T. Eto R. Fernandez Long Beach, CA 90822
1	Commander & Director David W. Taylor Naval Ship Research & Development Center Bethesda, MD 20084	3	ADTC/DLJW (Mr. W. Cook) MAJ. G. Spitale CAPT R. Bell Eglin AFB, FL 32542
2	Commander Naval Surface Weapons Center ATTN: Dr. W. G. Soper Mr. N. Rupert Dahlgren, VA 22448	4	ADTC/DLYV (Mr. J. Collins) Mr. J. Smith Mr. G. C. Crews Mr. J. L. Winger Eglin AFB, FL 32542
2	Commander Naval Surface Weapons Center ATTN: Dr. S. Fishman Silver Spring, MD 20084	1	AFML/LLN (Dr. T. Nicholas) Wright-Patterson AFB, OH 45433
9	Commander Naval Weapons Center ATTN: Code 31804, Mr. M. Keith Code 326, Mr. P. Cordle Code 3261, Mr. T. Zulkoiski Code 3181, John Morrow Code 3261, Mr. C. Johnson Code 3171, Mr. B. Galloway Code 3831, Mr. M. Backman Mr. R. E. Van Devender, Jr. Dr. O.E.R. Heimdalh China Lake, CA 93555	10	Battelle N. W. Laboratories ATTN: G. D. Marr PO Box 999 Richland, WA 99352
		1	Lawrence Livermore Laboratory PO Box 808 ATTN: Ms. C. Westmoreland Livermore, CA 94550
		2	Lawrence Livermore Laboratory PO Box 808 ATTN: Dr. R. Werne Dr. J. O. Hallquist Livermore, CA 94550

**DISTRIBUTION LIST**

<u>No. of Copies</u>	<u>Organization</u>	<u>No. of Copies</u>	<u>Organization</u>
6	<b>Los Alamos Scientific Lab</b> ATTN: Dr. R. Karpp Dr. J. Dienes Dr. J. Taylor Dr. E. Fugelso Dr. D. E. Upham Dr. R. Keyser P. O. Box 1663 Los Alamos, NM 87545	1	<b>Aeronautics Research</b> Associates of Princeton, Inc. 50 Washington Road Princeton, NJ 08540
5	<b>Sandia Laboratories</b> ATTN: Dr. R. Woodfin Dr. M. Sears Dr. W. Herrmann Dr. L. Bertholf Dr. A. Chabai Albuquerque, NM 87115	1	<b>Aerospace Corporation</b> ATTN: Mr. L. Rubin 2350 E. El Segundo Blvd El Segundo, CA 90009
1	<b>Headquarters</b> National Aeronautics and Space Administration Washington, DC 20546	1	<b>AVCO Systems Div</b> ATTN: Chang Sheng Ting 201 Lowell Street Wilmington, MA 01803
1	<b>Jet Propulsion Laboratory</b> ATTN: Dr. Ralph Chen 4800 Oak Grove Drive Pasadena, CA 91102	2	<b>Battelle Columbus Labs</b> ATTN: Dr. M. F. Kanninen Dr. G. T. Hahn 505 King Avenue Columbus, OH 43201
1	<b>Director</b> National Aeronautics and Space Administration Langley Research Center Langley Station Hampton, VA 23365	2	<b>Boeing Aerospace Company</b> ATTN: Mr. R. G. Blaisdell (M.S. 40-25) Dr. H.A. Armstrong ( MS 8C-23) Seattle, WA 98124
1	<b>U.S. Geological Survey</b> ATTN: Dr. D. Roddy 2255 N. Gemini Drive Flagstaff, AZ 86001	2	<b>Brunswick Corporation</b> ATTN: P.S. Chang R. Grover 4300 Industrial Avenue Lincoln, NE 68504
1	<b>Aerojet Ordnance Co.</b> ATTN: Dr. W. B. Freeman Dr. H. Wolfe 9236 East Hall Road Downey, CA 90241	1	<b>Computer Code Consultants, Inc.</b> ATTN: Dr. Wally Johnson 1680 Camino Redondo Los Alamos, NM 87544
		1	<b>Dresser Center</b> ATTN: Dr. M. S. Chawla P. O. Box 1407 Houston, TX 77001

DISTRIBUTION LIST

<u>No. of Copies</u>	<u>Organization</u>	<u>No. of Copies</u>	<u>Organization</u>
1	Effects Technology, Inc. 5383 Hollister Avenue Santa Barbara, CA 93111	4	Honeywell, Inc. Government and Aerospace Products Division ATTN: Mr. J. Blackburn Dr. G. Johnson Mr. R. Simpson Mr. K. H. Doeringsfeld 600 Second Street, NE Hopkins, MN 55343
2	Falcon R&D Thor Facility ATTN: Mr. D. Malick Mr. J. Wilson 696 Fairmount Avenue Baltimore, MD 21204	1	Hughes Aircraft Corporation ATTN: Mr. W. Keppel MS M-5, Bldg. 808 Tucson, AZ 85706
1	FMC Corporation Ordnance Engineering Div San Jose, CA 95114	1	International Applied Physics, Inc. ATTN: Mr. H. F. Swift 7546 McEwen Road Centerville, OH 45459
1	General Atomic Co. ATTN: R. M. Sullivan F. H. Ho S. Kwei P. O. Box 81608 San Diego, CA 92138	2	Kaman Sciences Corporation ATTN: Dr. P. Snow Dr. D. Williams 1500 Garden of the Gods Road Colorado Springs, CO 80933
1	General Dynamics ATTN: J. H. Cuadros P. O. Box 2507 Pomona, CA 91484	1	Lockheed Palo Alto Research Laboratory ATTN: Org 5230, Bldg. 201 Mr. R. Roberson 3251 Hanover Street Palo Alto, CA 94394
1	General Electric Company Armament Systems Dept. Burlington, VT 05401	1	Materials Research Lab, Inc. 1 Science Road Glenwood, IL 60427
1	President General Research Corporation ATTN: Lib McLean, VA 22101	2	McDonnell-Douglas Astro. Co. ATTN: Dr. L. B. Greszczuk Dr. J. Wall 5301 Bolsa Avenue Huntington Beach, CA 92647
1	Goodyear Aerospace Corporation 1210 Massillon Road Akron, OH 44315		
1	H. P. White Laboratory 3114 Scarboro Road Street, MD 21154		

**DISTRIBUTION LIST**

<u>No. of Copies</u>	<u>Organization</u>	<u>No. of Copies</u>	<u>Organization</u>
1	New Mexico Institute of Mining and Technology ATTN: TERA Group Socorro, NM 87801	1	US Steel Corporation Research Center 125 Jamison Lane Monroeville, PA 15146
1	Northrop Corporation ATTN: R. L. Ramkumar 3901 W. Broadway Hawthorne, CA 90250	1	VPI & SU ATTN: Dr. M. P. Kamat 106C Norris Hall Blacksburg, VA 24061
1	Nuclear Assurance Corporation ATTN: T. C. Thompson 24 Executive Park West Atlanta, GA 30245	2	Vought Corporation ATTN: Dr. G. Hough Dr. Paul M. Kenner P. O. Box 225907 Dallas, TX 75265
1	Pacific Technical Corporation ATTN: Dr. F. K. Feldmann 460 Ward Drive Santa Barbara, CA 93105	1	Westinghouse, Inc. ATTN: J. Y. Fan P. O. Box 79 W. Mifflin, PA 15122
1	Science Applications, Inc. 101 Continental Boulevard Suite 310 El Segundo, CA 90245	1	Drexel University Department of Mechanical Eng. ATTN: Dr. P. C. Chou 32nd and Chestnut Streets Philadelphia, PA 19104
1	Ship Systems, Inc. ATTN: Dr. G. G. Erickson 11750 Sorrento Valley Road San Diego, CA 92121	1	Forrestal Research Center Aeronautical Eng Laboratory Princeton University ATTN: Dr. A. Eringen Princeton, NJ 08540
1	Systems, Science and Software ATTN: Dr. R. Sedgwick P. O. Box 1620 La Jolla, CA 92038	3	Southwest Research Institute Dept of Mechanical Sciences ATTN: Dr. U. Lindholm Dr. W. Baker Dr. R. White 8500 Culebra Road San Antonio, TX 78228
2	TRW ATTN: U. Ausherman M. Bronstein One Space Park, R1/2120 Redondo Beach, CA 90277		
1	United Technologies Rsch Ctr ATTN: P. R. Fitzpatrick 438 Weir Street Glastonbury, CT 06033		

DISTRIBUTION LIST

<u>No. of Copies</u>	<u>Organization</u>	<u>No. of Copies</u>	<u>Organization</u>
4	SRI International ATTN: Dr. L. Seaman Dr. L. Curran Dr. D. Shockey Dr. A. L. Florence 333 Ravenswood Avenue Menlo Park, CA 94025	2	University of Delaware Dept of Mechanical Engineering ATTN: Prof. J. Vinson Dean I. Greenfield Newark, DE 19711
1	State University of New York at Stony Brook Department of Materials Science and Engineering ATTN: Dr. H. Herman Stony Brook, NY 11790	1	University of Denver Denver Research Institute ATTN: Mr. R. F. Recht 2390 S. University Blvd. Denver, CO 80210
2	University of Arizona Civil Engineering Department ATTN: Dr. D. A. DaDeppo Dr. R. Richard Tucson, AZ 85721	2	University of Oklahoma School of Aerospace, Mechanical and Nuclear Eng. ATTN: Dr. J. N. Reddy Dr. C. W. Bert Norman, OK 73019
1	University of Arizona School of Engineering ATTN: Dean R. Gallagher Tucson, AZ 85721	1	University of Vermont ATTN: C. Brown 201 Votey Bldg. Burlington, VT 05405
<u>Aberdeen Proving Ground</u>			
		Dir, USAMSA	
		ATTN: DRXSY-D	
		DRXSY-MP, H. Cohen	
		Cdr, USATECOM	
		ATTN: DRSTE-TO-F	
		Dir, USAMTD	
		ATTN: Mr. W. Pless	
		Mr. S. Keithley	
		Dir, USACSL, EA	
		ATTN: DRDAR-CLB-PA	
		Bldg. E3516	

### USER EVALUATION OF REPORT

Please take a few minutes to answer the questions below; tear out this sheet and return it to Director, US Army Ballistic Research Laboratory, ARRADCOM, ATTN: DRDAR-TSB, Aberdeen Proving Ground, Maryland 21005. Your comments will provide us with information for improving future reports.

1. BRL Report Number \_\_\_\_\_
2. Does this report satisfy a need? (Comment on purpose, related project, or other area of interest for which report will be used.)  
\_\_\_\_\_  
\_\_\_\_\_  
\_\_\_\_\_
3. How, specifically, is the report being used? (Information source, design data or procedure, management procedure, source of ideas, etc.)  
\_\_\_\_\_  
\_\_\_\_\_  
\_\_\_\_\_
4. Has the information in this report led to any quantitative savings as far as man-hours/contract dollars saved, operating costs avoided, efficiencies achieved, etc.? If so, please elaborate.  
\_\_\_\_\_  
\_\_\_\_\_  
\_\_\_\_\_
5. General Comments (Indicate what you think should be changed to make this report and future reports of this type more responsive to your needs, more usable, improve readability, etc.)  
\_\_\_\_\_  
\_\_\_\_\_  
\_\_\_\_\_
6. If you would like to be contacted by the personnel who prepared this report to raise specific questions or discuss the topic, please fill in the following information.

Name: \_\_\_\_\_

Telephone Number: \_\_\_\_\_

Organization Address: \_\_\_\_\_

\_\_\_\_\_  
\_\_\_\_\_